



Measuring the viscosity of lava in the field: A review

Magdalena Oryaëlle Chevrel, Harry Pinkerton, Andrew J.L. J.L. Harris

► To cite this version:

Magdalena Oryaëlle Chevrel, Harry Pinkerton, Andrew J.L. J.L. Harris. Measuring the viscosity of lava in the field: A review. *Earth-Science Reviews*, 2019, 10.1016/j.earscirev.2019.04.024 . hal-02150640v1

HAL Id: hal-02150640

<https://hal.science/hal-02150640v1>

Submitted on 7 Jun 2019 (v1), last revised 7 Mar 2023 (v3)

HAL is a multi-disciplinary open access archive for the deposit and dissemination of scientific research documents, whether they are published or not. The documents may come from teaching and research institutions in France or abroad, or from public or private research centers.

L'archive ouverte pluridisciplinaire **HAL**, est destinée au dépôt et à la diffusion de documents scientifiques de niveau recherche, publiés ou non, émanant des établissements d'enseignement et de recherche français ou étrangers, des laboratoires publics ou privés.

Measuring the viscosity of lava in the field: A review

Magdalena Oryaëlle Chevrel^{a*}, Harry Pinkerton^b, Andrew J.L. Harris^a

^aUniversité Clermont Auvergne, CNRS, IRD, OPGC, Laboratoire Magmas et Volcans, f-63000 Clermont-Ferrand, France

^bLancaster Environment Centre, Lancaster University, Lancaster LA1 4YQ, United Kingdom

*Corresponding author: oryaelle.chevrel@gmail.com

Abstract

Many scientists who have worked on active lava flows or attempted to model lava flows have recognized the importance of rheology in understanding flow dynamics. Numerous attempts have been made to estimate viscosity using flow velocities in active lava channels. However, this only gives a bulk or mean value, applies to channelized flow, and the need to estimate flow depth leads to a large degree of uncertainty. It is for this reason that some scientists resorted to more direct methods for measuring the lava viscosity in the field. Initial attempts used crude instruments (such as forcing a rod into a flow using the operators body-weight), and even the latest instruments (motor-driven rotational viscometer) are significantly less refined than those one would encounter in a well-equipped laboratory. However, if suitable precautions are taken during instrument design, deployment in the field and post-processing of data, the results form an extremely valuable set of measurements that can be used to model and understand the complex rheological behavior of active lava flows. As far as we are aware, eleven field measurements of lava rheology have been published; the first took place in 1948, and the latest (at the time of writing) in 2016. Two types of instrument have been used: penetrometers and rotational viscometers. Penetrometers are suitable for relatively high viscosity (10^4 - 10^6 Pa s) lava flows, but care has to be taken to ensure that the sensor is at lava temperature and measurements are not affected by the resistance of outer cooled crust. Rotational viscometers are the most promising instruments at lower viscosities (1 - 10^4 Pa s) because they can operate over a wider range of strain rates permitting detailed flow curves to be calculated. Field conditions are challenging and measurements are not always possible as direct approach to and contact with active lava is necessary. However it is currently the only way to capture the rheology of lava in its natural state. Such data are fundamental if we are to adequately model and understand the complex behavior of active lava flows.

Keywords

Lava flow, Rheology, Field Viscometry, Shear Stress, Strain Rate, Viscosity, Yield Strength, Penetrometer, Rotational viscometer

1 Introduction

Lava flow dynamics and flow length are influenced by a number of factors including effusion rate at the vent, ground slope, channel dimensions, flow velocity, eruption duration, insulation and, critically, the rheology of the lava (e.g., Walker 1973; Pinkerton and Wilson 1994; Keszthelyi and Self 1998; Griffiths 2000; Harris et al. 2005; Kerr and Lyman 2007; Harris and Rowland 2009; Castruccio et al. 2013). During an eruption, estimates of the effusion rate and mean ground slope can be made, and these can be used as source terms in lava flow emplacement models to assess potential hazards (e.g., Vicari et al., 2011; Ganci et al., 2012; Mossoux et al., 2016; Coppola et al., 2017). However, the rheological properties of the flowing and modeled lava are subject to major uncertainties. Current lava flow models (e.g., Crisci et al. 1986; Harris and Rowland 2001; Hidaka et al. 2005; A Vicari et al. 2007; Herault et al. 2009; 2011; Bilotta et al. 2014; Kelfoun and Vargas 2016; Chevrel et al. 2018a) use rheological data that are either unchanging during flow development or vary down flow as a function of evolving temperature and crystal content. However, these do not accurately reflect the behavior of lava during emplacement because they neglect the effects of volatile content, oxygen fugacity, cooling rate, degassing, strain rate and bubble growth.

Lava is composed of crystals and bubbles in suspension in a silicate liquid and its rheology depends on the viscosity of the liquid phase and on the effect of the particles (bubbles and crystals) it contains (cf. Pinerton and Stevenson 1992; Crisp et al., 1994; Cashman et al., 1999; Mader et al., 2013). The viscosity therefore changes down flow because lava temperature, bubble content and crystallinity evolve as functions of both time (i.e., as eruption progresses) and space (i.e., with distance from the source) (Lipman et al., 1985; Lipman and Banks, 1987; Moore, 1987; Crisp et al., 1994; Cashman et al., 1999; Soule et al., 2004; Riker et al., 2009; Chevrel et al., 2013; Robert et al., 2014; Rhéty et al., 2017). Upon eruption, the liquid phase is Newtonian and its viscosity depends on chemical composition (including major elements and volatiles) and temperature. The viscosity of silicate melts is relatively easily measured as a function of temperature in the laboratory and composition-based empirical models have been established (e.g., Bottinga and Weill, 1972; Shaw, 1972;

Hess and Dingwell, 1996; Giordano and Dingwell, 2003; Hui and Zhang, 2007; Giordano et al., 2008; Sehlke and Whittington, 2016). In contrast, the effect of particles is more difficult to quantify because the mixture becomes non-Newtonian and yield-strength, shear thinning and thixotropic behavior may appear. The mixture (melt + particles) rheology depends on particle concentration, aspect ratio (for crystals), ability to deform (for bubbles), size distribution, shear stress and applied strain rate (Barnes, 1989; Larson, 1999). The effect of particles has been estimated via several theoretical and empirical models based on experiments of analogue material (e.g., Einstein, 1906; Krieger and Dougherty, 1959; Maron and Pierce, 1956; Costa et al., 2009; Mueller et al., 2010; Castruccio et al., 2010; Cimarelli et al., 2011; Moitra and Gonnermann, 2015; Klein et al., 2018). These have been applied to constrain lava flow rheology in several studies (Pinkerton and Stevenson, 1992; Crisp et al., 1994; Cashman et al. 1999; Guilbaud et al., 2007; Harris and Allen, 2008; Riker et al., 2009; Chevrel et al., 2013; Le Losq et al., 2015; Castruccio and Contreras, 2016; Chevrel et al. 2016; Rhéty et al., 2017). The effect of crystals has also been explored through crystallization experiments of molten lavas (e.g., Ryerson et al. 1988; Pinkerton and Norton, 1995; Sato, 2005; Ishibashi and Sato, 2007; Vona et al., 2011; Vetere et al., 2013; Sehlke et al., 2014; Soldati et al., 2014; Chevrel et al., 2015; Kolzenburg et al., 2016, 2017) and by deformation of natural crystal-rich samples near the glass transition temperature (e.g., Caricchi et al., 2008; Champallier et al., 2008; Cordonnier et al., 2009; Avard and Whittington, 2012; Lavallée et al., 2012, 2007; Vona et al., 2013). The effect of bubbles on crystal-free lava rheology has been investigated using analogue material or theoretically (e.g., Stein and Spera, 1992; Manga et al., 1998; Lejeune et al., 1999; Saar and Manga, 1999; Bagdassarov and Pinkerton, 2004; Rust and Manga, 2002a; Llewellyn and Manga, 2005) as well as using bubble-bearing high viscosity silicate melts near the glass transition (Bagdassarov et al., 1994; Bagdassarov and Dingwell, 1993, 1992; Vona et al., 2016). The combined effect of bubbles and crystals has been studied via laboratory experiments on magmas (Bagdassarov et al., 1994; Pistone et al., 2016, 2013, 2012; Vona et al., 2017, 2016) and the three-phase theory (Phan-Thien and Pham, 1997; Harris and Allen, 2008). Although laboratory measurements are well controlled, they are not representative of field conditions because of differences in volatile content (dissolved and in the form of gas bubbles), oxygen fugacity and crystallinity changes during heating episodes in the laboratory. To generate realistic models of lava flow advance and to place laboratory measurements in reference to nature, we thus need a basic knowledge of the rheology of the molten mixture itself in its natural setting (i.e., in the field).

One method that is commonly used to obtain information on the rheological properties of lavas in the field involves measuring the post-emplacement dimensions of the flows (e.g., Hulme, 1974; Moore and Schaber, 1975; Fink and Zimbelman, 1986; Moore, 1987; Kilburn and Lopes, 1991; Wadge and Lopes, 1991). Most of these studies are based on the assumption that lavas can be approximated as Bingham fluids, and that their flow dimensions are controlled by the yield strength and plastic viscosity. However, post emplacement subsidence, complex lava flow fields and lava flow inflation may induce under- or over-estimation of flow viscosity using this method (e.g. Kolzenburg et al., 2018c). Another method involves measuring the mean velocity of lava in active channels to derive the rheological parameters. It is often assumed that the lava behaves as a Newtonian fluid and the flow has a parabolic velocity profile. In that case, the Jeffreys (1925) equation is applied to calculate the viscosity (e.g., Nichols, 1939; Krauskopf, 1948; Walker, 1973; Rose, 1973; Harris et al., 2004; James et al., 2007). Other studies showed that non-Newtonian flow behavior is preferable and consider a plug-flow model to extract yield strength and viscosity (e.g., Cigolini et al., 1984; Moore, 1987; Harris et al., 2002; Balmforth et al., 2007;). An additional field method can be used when flows undergo super-elevation when they encounter sharp bends in channels (Heslop et al., 1989; Woodcock and Harris, 2006). Unfortunately, there are few situations where this method can be applied. All these methods are based on the whole flow behavior, and therefore, suffer from potentially large uncertainties due to difficulties to measure channel shape, depth, lava density and underlying slope (cf. Hon et al., 2003; Lefler, 2011; Chevrel et al., 2013; Lev and James, 2014; Kolzenburg et al., 2018b). In addition, the calculated properties are not necessarily representative of the viscosity of the material itself but represent the behavior of the flow as a whole (fluid interior plus brittle and viscoelastic crust). Consequently, to constrain the rheological parameters of lava in its natural state, we must use field-based instrumentation.

The only way to directly establish lava rheology in the field is to measure it by inserting a viscometer into the flowing molten rock. If this technique is applied down an active channel and is combined with simultaneous temperature measurement and sampling, it is possible to capture the evolution of lava rheology as a function of cooling, degassing and crystallization. However, *in-situ* viscosity measurements are challenging due to the difficulty of approaching an active lava flow, and the problems of designing equipment that will make reliable measurements under such difficult conditions. Besides, during eruption, lava flows are continuously changing (advancing, cooling, degassing, advecting) therefore the

measurement timescales needs to be adapted with the timescale for which the lava is at constant conditions (mainly temperature). This is often a limitation for the measurements because low torques and low deformation rates are difficult to reach due to the fast thermal dynamics. As a result, only a small number of investigators have accepted the challenge of measuring the rheological properties in the field. Their studies are reported here. In this article, we thus review how rheological properties can be measured using field instrumentation. We then collate all field viscometry experiments made to date in chronological order. For each of these eleven cases found, we include a discussion of the field conditions, and instrument description, and review the main results and conclusions.

2 Measuring lava rheology in the field

2.1 Methods and theory

Quantification of rheology is described by the relationship between the applied stress, and the rate of deformation i.e. strain rate. These quantities are measured using a viscometer. There are essentially two types of viscometer that have been used to measure the rheological properties of lava in the field. One measures the resistance to penetration of an object, which moves into the lava, and the other measures the torque required to rotate a shear vane that is immersed in the lava. These viscometers are based on the principle of applying either a stress or a strain rate while measuring the response either of the strain rate or the stress. When using a rotational viscometer, the shear strain rate is a function of the rotation rate and the geometry of the vane. For a penetrometer it is a function of the penetrometer head shape and the axial penetration rate. Shear stress is a function of the torque acting on the rotating spindle or the force acting on the penetrating head. If the rotational viscometer or penetrometer has the ability to vary the speed of rotation or penetration, or the applied force, a graph of strain rate versus stress can be constructed to produce, following the term given by Lenk (1967), “flow curves”. Depending on the lava properties being measured, one of the following rheological models can be fitted to the data (see Chapter 5 in Chester et al., 1986). All parameters used for the following equations are given in Table 1.

For Newtonian behavior, the strain rate ($\dot{\gamma}$) is directly proportional to shear stress (τ). The proportionality coefficient is the viscosity (η) and is defined by:

$$\tau = \eta \dot{\gamma} \quad (1)$$

Bingham behavior is identified when a minimum stress (i.e., the yield strength, τ_0) needs to be overcome before deformation occurs. In that case, once the yield strength is overcome, the strain rate is proportional to shear stress. The proportional coefficient is the consistency (K), otherwise termed the Bingham or plastic viscosity. This is defined via:

$$\tau = \tau_0 + K\dot{\gamma} \quad (2)$$

When strain rate is not proportional to shear stress, and the lava has no discernible yield strength, the material is best characterized as a power law flow, defined as:

$$\tau = K\dot{\gamma}^n \quad (3)$$

where, if n , the flow index, equals unity this reduce to the Newtonian case (Eq.1).

The last rheological model used to describe lava behavior, is when a minimum stress is present and once it is overcome the shear stress follows a power law with strain rate. This is termed the Herschel-Bulkley model and described by:

$$\tau = \tau_0 + K\dot{\gamma}^n \quad (4)$$

For all fluids, the value of n in Eqs. 3 and 4, is evaluated graphically or numerically from the experimentally determined values of strain rate and shear stress. When $n > 1$, the fluid is dilatant (also termed shear thickening), i.e. viscosity increases with strain rate. Evidence for this behavior has been found in dykes (Smith, 1997, 2000), but has yet to be encountered in flowing lava. When $0 < n < 1$, the material is thinning with deformation, so that viscosity decreases with strain rate. In that case, the fluid follows a pseudo-plastic behavior. After a few percent of crystallization, it has been recognized that lavas preferentially follow this behavior (Pinkerton and Stevenson, 1992).

2.2 Instrumentation

2.2.1 Penetrometers

There are three types of penetrometer. A “simple” penetrometer is based on a penetrometer used for measurement of soil physical properties (Lunne et al., 1997) and is basically a metal rod, with a semi-spherical head, pushed into the lava. Penetrometers can be used to measure yield strength by establishing the minimum force required to initiate movement (Pinkerton and Sparks, 1978) or can be used to estimate viscosity by inserting the rod into the lava at a given constant force and recording the speed of penetration (Einarsson, 1949, 1966; Gauthier, 1973; Pinkerton and Sparks, 1978; Panov et al. 1988; Belousov and Belousova, 2018). Using

a semi spherical penetration head and assuming that the potential effect of lava sticking to the rod is negligible, the viscous drag is equal to half of Stokes' force acting on a sphere penetrating through a viscous medium (Panov et al., 1988; Belousov and Belousova, 2018). The lava viscosity is then calculated via:

$$\eta = \frac{F}{3\pi u R_{eff}} \quad (5)$$

where F is the force of penetration (viscous drag), u is the speed of penetration, and R_{eff} is the effective radius of the rod. The force is recorded by a hand gauge and the velocity is measured from the penetration depth and time to reach that depth. This results in a single viscosity measurement point, which is averaged over the duration of penetration. For a given penetration depth the viscosity may then be obtained from prior calibration (Einarsson, 1966, 1949; Gauthier, 1973; Pinkerton and Sparks, 1978).

The second type of penetrometer is termed "ballistic" penetrometer as used by Gauthier (1971, 1973). This technique involves shooting a spear at high-speed perpendicularly into the lava and measuring its penetration depth. The viscosity is then calculated based on previous laboratory calibrations using the same spear on various liquids of different viscosities. The high initial penetration velocity prevents lava advance rates from influencing the measurement and limits cooling of the lava around the spear during penetration. The major disadvantage of such penetrometers is that they are inserted through the outer, cooled part of a flow, thus the force required to penetrate the lava is the result of a summation of shear stresses induced within the thickness penetrated, the major resistance to shearing being due to the more viscous outer (crusted) regions. This penetrometer thus tends to give a semi-quantitative measurement of the shear strength of the cooler exterior of a flow, and little indication of the rheological characteristics of the hot interior.

This problem can be overcome using a third type of penetrometer that is first preheated and inserted through the cooled outer regions before being activated, so only the nose of the penetrometer that had been placed into the flow interior is moved forward (Pinkerton and Sparks, 1978). This instrument used a compressed spring as the energy source for penetration. The controlled reduction in axial force during penetration was recorded, together with the simultaneous piston advance rates. This type of dynamic penetrometer permitted the shear stress - strain rate characteristics of the lava to be determined using the method outlined in Pinkerton (1978).

219

Symbol	Description	Unit
η	Viscosity	Pa s
τ	Shear stress	Pa
$\dot{\gamma}$	Strain rate	s ⁻¹
τ_0	Yield strength	Pa
K	Consistency	Pa s
n	Flow index	
<i>Penetrometer</i>		
F	Force of penetration	N
u	Speed of penetration	m s ⁻¹
R_{eff}	Effective radius of the rod	m
<i>Rotational viscometer</i>		
M	Torque	N m
Ω	Angular velocity	rad s ⁻¹
h	Vane length	m
R_i	Vane radius	m
R_o	Container radius	m

220 **Table 1:** Notation of parameters and units

221

222 2.2.2 Rotational viscometer

223 Rotational viscometers involve a rotating spindle immersed into the molten lava. Two types
224 of rotational viscometer have been employed in the field: a fixed rig sited on the top of a lava
225 lake (Shaw et al., 1968) and a portable instrument inserted by hand through the flow surface
226 and into the lava interior (Pinkerton, 1994; Pinkerton et al., 1995a, 1995b; Pinkerton and
227 Norton, 1995; Chevrel et al., 2018a). In use, the spindle can be operated in either controlled
228 strain rate or controlled shear stress mode. The theory employed with this instrument is that of
229 wide-gap concentric cylinder viscometry where the torque is converted into shear stress and
230 the rotational speed into strain-rate using the spindle geometry via the Couette theory, which
231 is similar to the theory used for the laboratory viscometers described in Dingwell (1986) and
232 Spera et al. (1988). Unlike most laboratory experiments where the immersed spindle is
233 cylindrical, vane geometry is commonly used in the field to lower the weight, ease
234 penetration, reduce disturbance of lava during insertion, minimize the effects of cooling and
235 reduce slippage between the edge of the vane and the lava. The material between the vanes is
236 trapped and therefore a virtual cylinder of sample material is used for the calculation. The
237 shear stress is then calculated via:

$$\tau = \frac{M}{2\pi h R_i^2} \quad (6)$$

where M is torque, h is vane length and R_i is the radius of the rotating cylinder (or equivalent radius of the vane). The strain rate is obtained from the angular velocity of the rotating vane via (Stein and Spera, 1998):

$$\dot{\gamma} = \frac{2\Omega}{n \left(1 - \left(\frac{R_i}{R_o} \right)^{2/n} \right)} \quad (7)$$

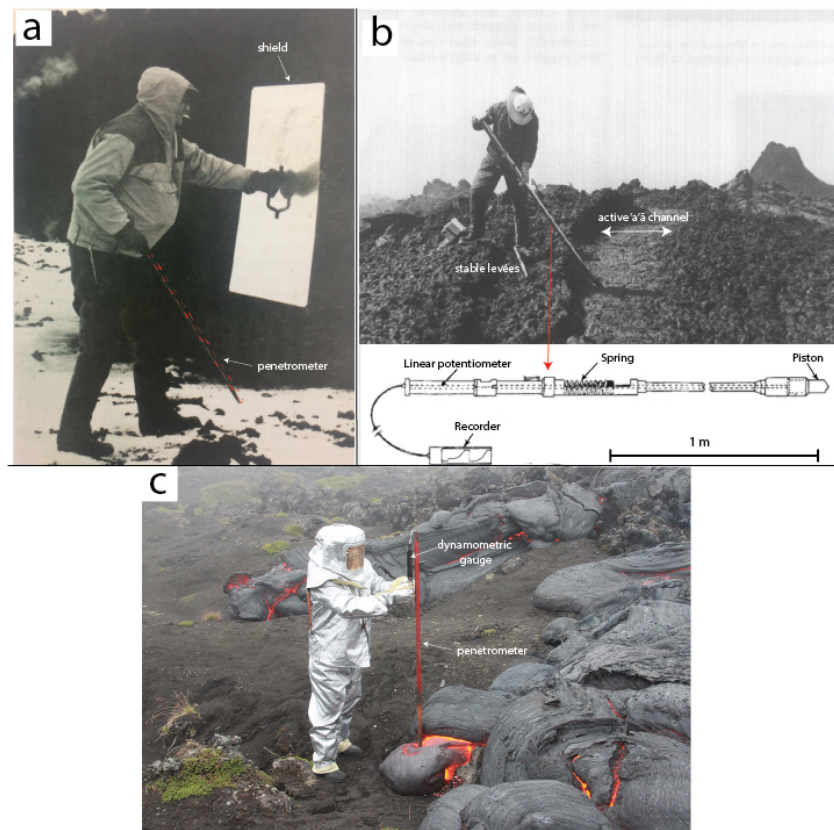
where Ω is angular velocity, n is flow index (obtained by calculating the slope of the measured $\ln(\tau)$ against $\ln(\Omega)$), and R_o is the radius of the outer cylinder.

3 Review of lava viscometry experiments in the field

3.1 An iron rod thrust into the lava by Einarsson (1949) at Hekla, Iceland

While observing lava emplacement on Hekla in 1948, Einarsson quickly realized that the lava presented interesting changes in vesicularity, temperature, crystallinity and apparent viscosity (Einarsson 1949). To measure viscosity, he used a simple iron rod and thrust it by hand into the lava. Einarsson applied a force on the rod manually and measured the time needed to penetrate the lava. From a qualitative approach, he could “feel” different behaviors. The most fluid lava allowed him to push the iron rod in with one hand, which reached depth of 20 to 30 cm in one or two seconds. In the most viscous lava, he could thrust the rod only 2-3 cm into the flow (also in 1 to 2 s) and this was achieved by putting his whole body weight onto the rod. To quantify viscosity, back into the laboratory, Einarsson established a relationship between viscosity and velocity of penetration from repeated measurements using the iron rod plunged into a hot mixture of Trinidad asphalt and asphalt oil. He estimated the viscosity of the lava at Hekla to be between 5×10^4 Pa s and 1.5×10^6 Pa s, and he estimated an error of about half order of magnitude. The erupted lavas were basaltic-andesite (55 wt.% SiO_2) and were described as ‘a’ā to block type. The maximum temperature was estimated using an optical pyrometer as 1150°C (Einarsson 1949). Analyses of the lava texture revealed that the low viscosity values corresponded to “spongy, uncrystallized fluid”, while the high viscosity value corresponded to denser lava. Einarsson (1949) concluded that accurate measurements of viscosity using this technique on this type of lava are difficult because of the lack of time available to make instrumental measurements and because of hazards arising from blocks

264 falling from the steep rubbly flow margin and high radiant heat. In 1961, Einarsson intended
 265 to measure the lava viscosity at Askja (Iceland; Fig. 1a) but no data were recorded.



266
 267 **Figure 1:** a) Einarsson holding the penetrorometer in one hand and a shield in another hand, advancing toward
 268 the lava flow during Askja (Iceland) eruption in 1961 (photo modified from Solbnes et al. 2013). b) Pinkerton
 269 using the penetrorometer Mark 2 on a small channelized 'a'ā flow of Mont Etna (Italy) in 1978 (sketch modified
 270 from Pinkerton and Sparks, 1978). c) Belousov using a lava-penetrorometer equipped with a dynamometric gauge
 271 on a pāhoehoe lobe during the Tolbachik (Russia) eruption in 2013 (modified from Belousov and Belousova
 272 2018).

273 3.2 Viscosity measurement at Surtsey, Iceland, by Einarsson (1966)

274 During the Surtsey eruption in 1964, Einarsson measured the viscosity of the flowing lava
 275 using the same approach as he applied at Hekla in 1948 (Einarsson 1966). Einarsson
 276 mentioned that this time the measurements were difficult to perform because the lava was too
 277 fluid. Because the penetrorometer was pushed by hand, it was difficult to regulate the force of
 278 penetration to a minimum in order to measure the resistance of the fluid lava. After several
 279 attempts, Einarsson estimated that the penetrorometer moved 10 cm vertically into the lava at
 280 the front of a lava lobe under its own weight in 0.5 s from which he obtained a viscosity
 281 estimation of 5×10^2 Pa s. Einarsson noticed that this value was lower than expected because
 282 he estimated viscosity at 10^3 Pa s from lava wave amplitudes in the lava lake located over the

vent. This underestimation was attributed to the “foamlike” texture of the lava. At that time, Einarsson therefore sensed the potential effect of bubbles on lowering lava viscosity. The samples of spatter that he collected showed about 45 vol. % of vesicles and 40 vol. % of crystals (feldspar and olivine). The maximum temperature measured in the field with an optical pyrometer was 1140 °C. Given these thermal and textural characteristics, a viscosity value of 5×10^2 Pa s seems, therefore, appropriate.

3.3 Viscosity measurements performed by Shaw et al. (1968) at Makaopuhi lava lake, Hawaii

Shaw et al. (1968) used the rotational viscometry method to determine the rheological properties of lava at Makaopuhi lava lake in March 1965. Makaopuhi lava lake formed in 10 days by eruption of lava into a pit crater forming an 85 m deep and 800 m wide “pond”, and after which the surface became stable and the upper part began to solidify. When the crust reached a thickness of 2 m, cores were drilled periodically for temperature measurements and lava sampling, as described in Wright and Okamura (1977). The viscosity measurements were performed using one of the drill holes once the crust reached a thickness of about 4 m. The experimental setup consisted of a support stand fixed on the top of the solidified lava lake surface. A shaft, with a vane attached to its lower end, was suspended from the stand and lowered vertically into the lava (Fig. 2). A casing was employed allowing the shaft to reach the molten lava at the bottom of the cooled crust, where the temperature reached its maximum (Fig. 2). A wire was spooled to the shaft, passed through a pulley and attached to a load, permitting the shaft to rotate. In this way, by changing the load weight, different torques were applied to the rotating vane. Flow curves were obtained by measuring the resulting rotational speed (using stopwatches). The setup had been previously calibrated using petroleum asphalt and uncertainties of 20 % on the viscosity were obtained. In the field, four different loads were applied at two different depths (position 1 at 6.8 m and position 2 at 7.5 m) using the same vane (Fig. 2). The temperature was measured at $1130 \pm 5^\circ\text{C}$ and sample analyses revealed < 5 % vesicles and 25 % of crystals. Viscometry results indicated that the lava was non-Newtonian and thixotropic, which means that they observed a hysteresis between values acquired during increasing and decreasing load (“up” and “down” curves, i.e. the “down” stress-strain-rate path does not match the “up” path). Considering the up-curves, Shaw et al. (1968) established that the Bingham model was the most appropriate to fit their data. They estimated the yield strength to be 120 and 70 Pa, and obtained a plastic viscosity of 6.5×10^2 and 7.5×10^2 Pa s, for positions 1 and 2, respectively over strain rates $0.1 - 1 \text{ s}^{-1}$. These

compare with values of 80 to 115 Pa s obtained for the lake interior by Wright and Okamura (1977) by applying Stokes' Law to olivine crystal setting; the difference is likely due to the latter estimate being for melt only and the former for a melt-crystal mixture. A re-analysis of the Shaw et al. (1968) data suggested that no yield strength was present and that power law models in the form of $\tau = 974 \dot{\gamma}^{0.75}$ and $\tau = 716 \dot{\gamma}^{0.54}$ provided a better fit with positions 1 and 2, respectively (Heslop et al., 1989).

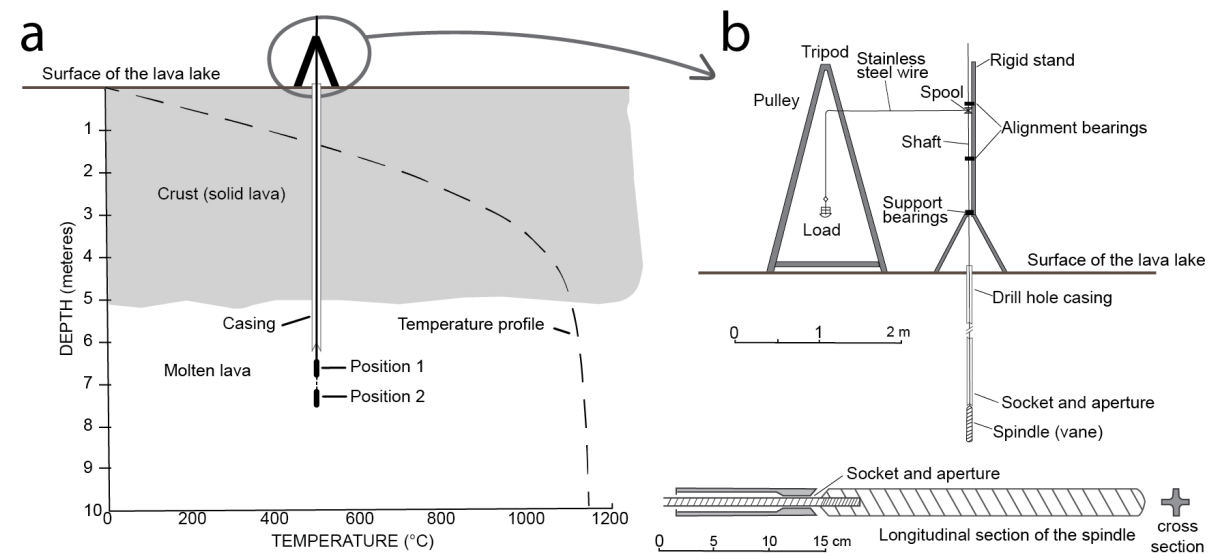


Figure 2: Set-up of the viscosity measurements performed by Shaw et al. in 1968 at Makaopuhi lava lake, Hawaii. Modified from Shaw et al. 1968. a) Schematic view of the stand fixed onto the top of the solidified lava surface (thickness of the crust was of about 4-5 m at that time) showing the two positions where measurements were performed and the temperature profile; b) zoom of the rotating viscometer device and spindle.

Shaw et al. (1968) also performed a falling sphere experiment. This experiment consisted of a steel sphere attached to a fine stainless steel wire that passed through the same casing used for the rotational viscometer. The sphere was released into the lava at its hottest part and the movement of the wire behind the descending sphere provided information to calculate the viscosity. However, they obtained only one measurement because in all other attempts the wire broke before a measurement was taken. The apparent viscosity they obtained via Stokes Law was 6×10^4 Pa s for a strain rate of 0.004 s^{-1} . Although this is larger than values calculated using the power law models, it is consistent with pseudo-plastic behavior.

These pioneering viscosity measurements are of uncontestably good quality. However the technique employed is appropriate only for stable lava lake with a thick crust. Employment beyond such a setting is therefore limited.

3.4 A shooting spear to measure lava viscosity on Mount Etna, Italy, by Gauthier (1973)

During the eruption of Mount Etna between 1969 and 1971, Gauthier (1971, 1973) performed viscosity measurements using a crossbow to fire a ballistic penetrometer (a stainless steel spear), into the lava flow. The penetrometer had an initial speed of 22 m/s. Based on calibration, viscosity is determined from the final depth of penetration. The relation between viscosity and penetration depth was established from laboratory experiments on materials with different viscosities. The penetration depth was directly read from graduations on the spear. In May 1971, Gauthier performed three sets of measurements. The first set was completed during the first phase of the eruption at the lava flow front, 500 m from the vent. Here, the viscosity was measured to be $\sim 1 \times 10^3$ Pa s and the temperature was 1050 °C. Measurements on several incandescent blocks yielded $\sim 2.2 - 5.7 \times 10^3$ Pa s at a temperature of 1080 °C. For other blocks, where the surface viscosity was clearly higher, estimates of more than 10^7 Pa s were obtained for the outer few centimeters, $\sim 4.3 \times 10^3$ Pa s at 13 cm and $\sim 8.5 \times 10^2$ Pa s at 33 cm. The second set of measurements, completed at the end of the first eruptive phase at the vent resulted in a viscosity of $\sim 1.1 - 6.3 \times 10^5$ Pa s at a temperature of 1090 ± 14 °C. The third set of measurement was made at the beginning of the second eruptive phase near the vent. Here, a temperature of 1128 °C and viscosity of $\sim 1.7 - 2.4 \times 10^3$ Pa s was measured. A sample collected near the vent from a depth of 50 cm was analyzed. The lava was a trachy-basalt with 44.6 vol.% of crystals, 22.8 vol.% of glass and 32.6 vol.% of bubbles.

Although viscosity values were obtained from these measurements, Gauthier (1973) concluded that “the objections to this method do not arise from difficulties of its application in the field conditions, but from rheological interpretation of the length of penetration”. Indeed, although the calibration fluids used in the laboratory had a vertical viscosity gradient between the upper layer and the material core, they did not represent the same gradient as natural lava. In other words, it was extremely difficult to calibrate the method by using a similar viscous gradient to that found in a lava flow.

Gauthier (1971) also designed a simple penetrometer, which included a dynamometric gauge and a thermocouple at the rod end. This instrument, when associated with video footage, would allow measurement of the temperature of the lava and its viscosity as deduced from the rate and depth of penetration. He believed that this rather simple and light-weight method was well adapted for fieldwork. Unfortunately, it was never built.

3.5 Field measurements of rheology of lava by Pinkerton and Sparks (1978) at Mount Etna, Italy

Pinkerton and Sparks (1978) deployed three instruments to characterize the rheological properties of the lava flows erupted at Mount Etna during the 1975 eruption. The most sophisticated was the “Mark 2” field viscometer. The Mark 1 was considerably heavier than the Mark 2 and was used only once during the 1973 eruption on Heimaey—with limited success. It had two large (~100 mm diameter) pistons moving out of an even larger cylinder that was inserted into the flow. It was extremely cumbersome and difficult to use, and preheating it was a major issue. However, parts of the Mark 1 instrument were used in the construction of the Mark 2.

The Mark 2 instrument was designed to overcome the problems with previous penetrometer methods. The penetrometer’s head was protected from the cooler crust through which it passed by an outer stainless steel tube. Once it had passed through the thermal boundary layer and reached thermal equilibrium with the surrounding lava, it was propelled into the flow by a compressed spring. This resulted in a gradually decreasing axial force being applied and hence a decreasing shear stress being applied to the isothermal region adjacent to the advancing piston (Fig. 1b). The position of the piston and hence velocity was recorded using a hot wire pen recorder. On each occasion that the viscometer was used, the piston did not extend fully, indicating that the lava had a measurable yield strength. Prior to field deployment, the instrument had been calibrated in a viscous sucrose solution. The method used to calculate the rheological properties is detailed in Pinkerton (1978). This first instrument was employed 3 m down flow from the active vent. Measurements were made at a depth of 20 cm where the temperature was 1086 ± 3 °C and the crystallinity of the flow interior was 45 vol.%. More than 20 data points were obtained for shear rates < 0.15 s⁻¹. The results indicated that the lava behaved in a pseudo-plastic manner, though it could be approximated to a Bingham fluid at the applied shear rates. The best fit revealed a yield strength of 370 ± 30 Pa and a plastic viscosity of $9.4 \times 10^3 \pm 1.5 \times 10^3$ Pa s.

The second instrument employed was a conventional penetrometer, which comprised a 2 m long, 3 cm diameter stainless steel rod. A pressure transducer allowed the axial force during insertion to be measured. This instrument was used in a dynamic mode by measuring the time taken by the pre-heated penetrometer to move 10 cm when inserted into the flow interior under a range of applied axial forces. Methods used to calibrate this instrument and to calculate rheological properties were similar to those used for the Mark 2 viscometer

(Pinkerton, 1978). One apparent yield strength measurement of 860 Pa was made at the same point as the Mark 2 viscometer. This value is higher than the previous measurement due to shear along the length of the shaft in contact with the outer thermal boundary layer and confirms the limitations of simple penetrometers. Another yield strength measurement made at a depth of 10 cm inside an advancing flow front was 6500 Pa at a temperature of 1045 °C.

The final instrument used was a stainless steel shear vane attached to a torque wrench that allowed yield strength to be measured by slowly applying torque until the shear vane began to rotate. The vane was preheated to lava temperature and inserted into the isothermal core to avoid the effects of the cooler flow margins. To minimize the effects of shearing by the cooler flow on the shaft, a ‘dummy end’ was used at each location. Additionally, the measured torque required to initiate movement of the shaft at the same immersion depth without the vane was subtracted from the torque with the vane attached. This instrument was used at eight locations on two lava flows at different distances from the vent. The results indicated that the yield strengths measured using the torque wrench were compatible with the values obtained with the Mark 2 viscometer. Values increased from 6.05×10^2 Pa at 1083 °C, close to the vent, to 1.4×10^3 Pa at 1080 °C, 7 m down flow and 2×10^3 Pa at 1070 °C, 24 m down flow from the vent. These measurements demonstrate the potential to make systematic measurements down an active flow.

3.6 Simple penetrometer employed at Klyuchevskoy, Russia, by Panov et al. (1988)

During the 1983 Predskazannyi eruption at Klyuchevskoy volcano, Panov et al. (1988) employed a simple penetrometer (Panov et al., 1985 in Russian, later translated into English by Panov et al., 1988). The instrument was a steel pole, 14 mm in diameter and 2 m long, with a rounded end. Viscosity was estimated from the measurement of the speed at which the rod penetrated the lava under a known force and by assuming that the viscous drag was equal to half of Stokes’ force (Eq. 5). In practice, the penetration speed was measured from the time interval between the submersion of marks noted on the rod. The force acting on the rod was the combined weight of the rod itself and the muscular effort applied. The rod was not preheated, therefore when it was plunged into the lava a chilled margin formed around it. To correct for this effect, Panov et al. (1988) added 1 to 2 mm to the rod diameter for the calculation of viscosity. During measurements, the penetration rate did not change under constant applied force, independently of the depth of penetration. The viscosity was measured to be between 1.1×10^4 Pa s and 3.6×10^5 Pa s. No systematic variation was observed with distance from the vent to the measurement location (15 to 35 m). Panov et al. (1988) noticed

the similarity (within an order of magnitude) of the penetrometer results with estimation of viscosity obtained using the Jeffreys (1925) equation. No data on the lava chemistry and crystal and bubble content was given.

3.7 Vane rotated by hand to measure viscosity of Mount Etna 1983 lava flow by Pinkerton and Norton (1995)

Pinkerton and Norton (1995) presented results of viscosity measurements performed during the eruption of Mount Etna in 1983. These viscosity measurements were performed using a rotating vane system on a breakout from the main channel where the measured temperature was 1095 °C. The vane was pre-heated and then inserted into the lava and rotated at different rates by hand (Fig. 3a). The system was equipped with a torque meter to measure the torque required to rotate the vane and rotation speeds were monitored with an optical tachometer. Four data points were acquired before the lava began to develop an impenetrable crust. In view of the limited range of rotation rate (5 – 9 rad/s), no unique rheological model could be applied. Assuming Newtonian behavior, the viscosity was calculated to be 1.385×10^3 Pa s. Applying a Bingham model, the yield strength was 3.7×10^2 Pa with a plastic viscosity of 1.26×10^3 Pa s and at unit strain rate the apparent viscosity is 1.63×10^3 Pa s. This range of values was consistent with those measured in the laboratory on melted samples from the same lava flow (Pinkerton and Norton, 1995, 1983). The lava was a trachy-basalt but unfortunately crystal and bubble content was not given. However, field viscosity values are in close agreement with those measured at the same temperature in the laboratory at for crystal content between 30 and 40 vol. %.

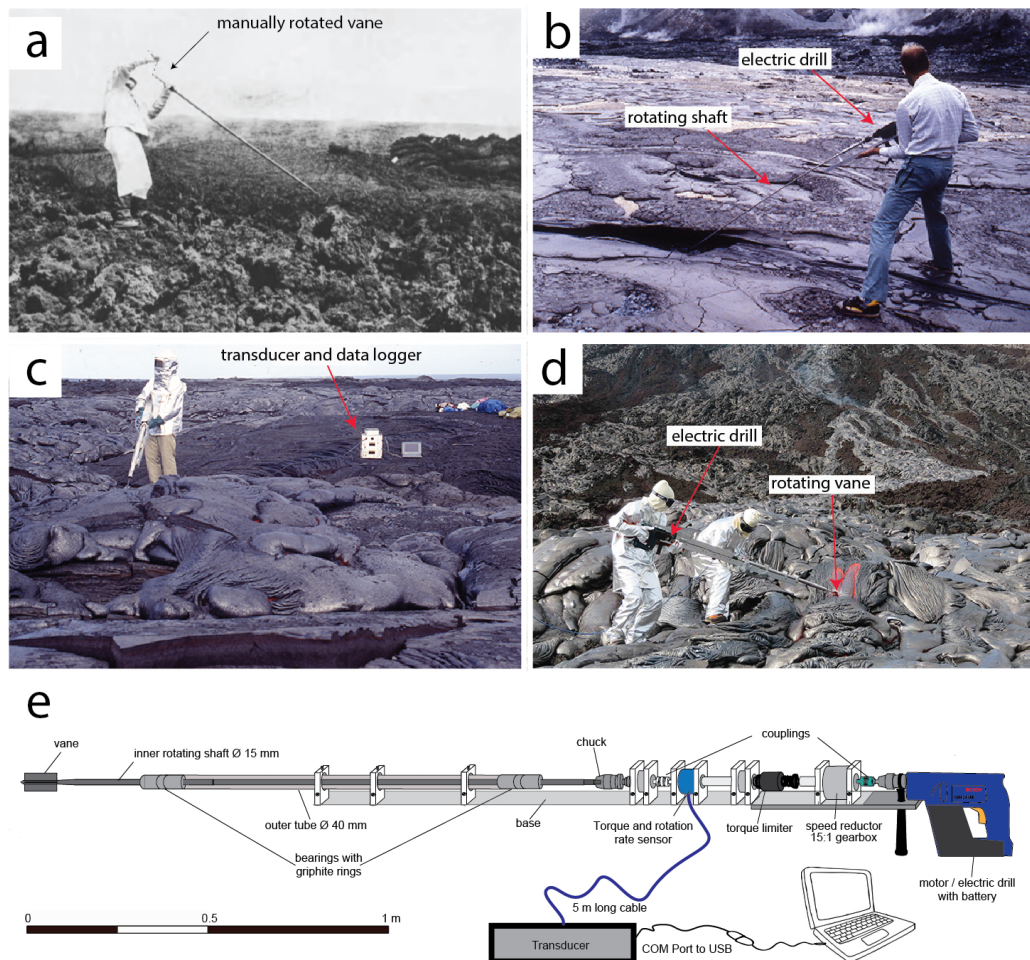


Figure 3: Rotational viscometers: a) Pinkerton taking rheological measurements in 1983 at Mount Etna using a manual shear vane (Chester et al., 1986) ; b) Pinkerton in 1988 at Oldoinyo Lengai using the first motor-driven shear vane (Pinkerton et al. 1995); c) Pinkerton et al. (1994) at Kilauea holding the new version of the motor-driven rotational viscometer: d) Chevrel et al. (2018b) using the refurbished viscometer in 2016 at Kilauea. e) Schematic representation of the refurbished viscometer, modified from Chevrel et al. (2018b)

3.8 Portable rotational viscometer to measure the viscosity of carbonatite at Oldoinyo Lengai, Tanzania, by Pinkerton et al. (1995a)

Rheological field measurements performed in November 1988 on natrocarbonatite lavas at Oldoinyo Lengai by Pinkerton et al. (1995) (Fig. 3b) were made using a motor-driven version of the equipment used on Etna in 1983. A 24-V DC Bosch drill was used to drive a vane at different, constant, rotation rates, which were measured using an optical tachometer. Torques corresponding to different rotation rates were measured using a torque meter that was mounted coaxially between the drive mechanism and the vane. This set of measurements revealed that the vesicle-free natrocarbonatite lavas behaved as inelastic Newtonian fluids with viscosities ranging from 1 to 5 Pa s. In contrast, highly vesicular lavas had apparent

viscosities of $0.7 - 1.2 \times 10^2$ Pa s at a strain rate of 1 s^{-1} and apparent viscosities of $0.3 - 3$ Pa s at a strain rate of 3 s^{-1} . These measurements were slightly higher than those measured subsequently in the laboratory by Norton and Pinkerton (1997) who concluded that these differences arose from differences in vesicularity and volatile contents between laboratory and field measurements.

3.9 Portable rotational viscometer to measure the viscosity of pāhoehoe lobes at Kilauea, Hawaii, by Pinkerton et al. (1995b)

Pinkerton (1994) and Pinkerton et al. (1995b) performed rheological measurements on small pāhoehoe lobes erupted at Kilauea in September 1994 using a new rotational portable viscometer based on the prototype employed at Oldoinyo Lengai. The viscometer was driven by a 24-V DC Bosch drill motor connected to a (15:1) reduction gearbox, a torque limiter and a torque-rotation rate sensor (Fig 3c). The sensor (DORT Optical rotary torque transducer from Sensor Technology Ltd) was linked via a transducer to a data logger. After each set of measurements, raw rotation rate and torque data were downloaded to a laptop and later processed with custom software. The main drive shaft was protected from the cooler outer layer of the flow by an outer tube with bearing assemblies (containing graphite rings to minimize friction) at regular intervals. This helped to maintain alignment of the inner shaft. Three pāhoehoe lobes (20 to 50 cm thick) were measured, each of which had maximum internal temperatures of 1146°C . All lavas measured had properties that could be approximated by a pseudoplastic power law model with plastic viscosity ranging from 2.3 to 5.5×10^2 Pa s and with corresponding power law exponents of 0.77 and 0.53, respectively. Pinkerton et al. (1995b) concluded that the higher viscosities resulted from lava with higher crystallinity and bubble content, but quenched samples collected following each measurement were not analyzed until the present study when one sample was analyzed (see appendix). The lava can be classified as porphyritic basalt with 4 vol.% of olivine phenocrysts and 12 vol.% of microlites (olivine + plagioclase + clinopyroxene) within a glassy matrix (55.1 wt. % SiO_2 and $\text{Mg} \# = 48$). The vesicle content was measured at 34 vol. % from image analyses and from density-derived measurements. The viscosity of the interstitial liquid was calculated from the glass composition (including 0.07 wt. % H_2O) using the model of Giordano et al. (2008) at 1146°C . The effect of crystals and of bubbles on viscosity was estimated following the methods of Mader et al. (2013) and Llewellyn and Manga (2005), respectively. Considering deformable bubbles (capillary number >1 for the strain rates applied during the measurements), the viscosity is estimated at 3.5×10^2 Pa s, which is in agreement with the

field measurements at unit strain rate. Unfortunately no other sample could be analyzed to examine whether from one lobe to another the texture was different so as to explain the range of viscosities measured.

3.10 Viscometry using a simple penetrometer on pāhoehoe lobes at Tolbachik, Russia, by Belousov and Belousova (2018)

In 2013, during the Tolbachik eruption, Belousov and Belousova (2018) performed viscosity measurements on several pāhoehoe lobes using a simple penetrometer (Fig. 1c) based on the method of Panov et al. (1985). In these experiments, Belousov and Belousova measured penetration rate of the rod as it passed through the pāhoehoe lobe producing a viscosity profile from the lobe top to the base (a distance of 10 to 25 cm). The speed of penetration was measured via video footage where marks on the penetrometer were tracked on each frame. The force of penetration was applied manually and recorded using a spring balance. Repeated measurements on each lobe and/or neighboring lobes (about 20 in total) gave interior viscosities between 5×10^3 and 5×10^4 Pa s. The viscosity of the upper and basal section of the lobes was measured as high as 6×10^4 to 4×10^5 Pa s. Measurements performed at various distances from the vent resulted in constant viscosity. The 'a'ā flow type could not be measured because of the impenetrable crust. Where the measurements were performed, maximum temperatures of 1082 °C were recorded with a K-type thermocouple at depths of several centimeters. The authors did not sample the lava at the moment of the measurements, but reported the chemical and textural analyses of previous studies. The lava was sub-aphyric basaltic trachyandesite (52 wt. % SiO₂) with 25 to 43 vol.% of crystals (mainly plagioclase and olivine) and 6 vol.% of vesicles (Plecho et al., 2015). Plecho et al. (2015) estimated the lava viscosity at $0.9 - 2.8 \times 10^3$ Pa s from chemical and textural characteristics. They used the model of Bottinga and Weill (1970) at 1100 °C for the melt viscosity and the Einstein-Roscoe model for the effect of crystals. As noted by Belousov and Belousova (2018), this estimate is in good agreement with their field viscosity measurements of the most fluid part of the pāhoehoe lobes. Recently, Ramsey et al. (2019) also estimated the viscosity from textural and chemical data given by Plecho et al. (2015) but using Giordano et al. (2008) for the interstitial melt viscosity at 1082°C. This revealed a slightly higher viscosity of 1.9×10^4 Pa s, which is in better agreement with the Belousov and Belousova (2018) measurements.

3.11 Portable rotational viscometer to measure the viscosity of pāhoehoe lobes of the 61G lava flow at Kilauea, Hawaii by Chevrel et al. (2018b)

In 2016, Chevrel et al. (2018a) used the same instrument as Pinkerton et al. (1995b) but it was refurbished and equipped with a different torque sensor (TORQSENSE E300 from Sensor Technology Ltd), communication system and new vanes. Tests in the laboratory using a calibrated viscosity standard, showed that the instrument could measure absolute viscosity with less than 5 % error, but was limited to strain-rates $> 0.6 \text{ s}^{-1}$ and torque measurements above $3 \times 10^2 \text{ Pa}$. Chevrel et al. carried out measurements on pāhoehoe lobes from the 61G lava flow of Kilauea's Pu'u 'Ō'ō eruption (Fig. 3d). A Newtonian viscosity of $3.8 \times 10^2 \text{ Pa s}$ was measured for strain-rates $> 1 \text{ s}^{-1}$ and at 1144 °C . No yield strength was measured indicating that yield strength, if present, must be below the 300 Pa measurement limit of the device. In contrast to Pinkerton et al. (1995b), low strain rates could not be measured (due to torque sensor sensitivity). The data could be fitted with a power law model of the form $\tau = 424 \dot{\gamma}^{0.88}$ but with a low fit coefficient of 0.79. Chevrel et al. also collected samples by quenching the lava attached to the share vane and completed textural and petrographic analyses, which allowed quantification of the effect of each phase on viscosity. The viscosity of the interstitial liquid was calculated from the glass composition (including 0.07 wt. % H_2O) using the model of Giordano et al. (2008). The effect of crystals (16 vol. %) and of bubbles (50 vol. %) on viscosity was estimated following the methods of Mader et al. (2013) and Llewellyn and Manga (2005), respectively. Considering deformable bubbles (capillary number was calculated > 1), the results gave a viscosity of $2.2 \times 10^2 \text{ Pa s}$, in agreement with the field measurements. Considering the bubbles to be rigid spheres resulted in an overestimation of the viscosity by one-to-two orders of magnitude.

4 Discussion

4.1 Field viscometers

Penetrometers have been employed to measure lava's rheological properties from the first published measurement by Einarsson (1948) until recently (Belousov and Belousova, 2018). This instrument has been favored because it is light, easy to build (it consists of a rod equipped with a dynamometric gauge) and permits quick estimates of the lava viscosity within a wide range ($10^3 - 10^6 \text{ Pa s}$; Figure 4). However, as highlighted by Einarsson (1966), the penetrometer is not well adapted for low viscosity lava ($< 10^3 \text{ Pa s}$) because it sinks too

rapidly into the lava. Additionally, simple penetrometers do not allow rheological flow curves to be calculated because strain rate cannot be varied at the same position (viscosity is estimated from penetration velocity). Furthermore, unless the rod has been pre-heated, or meticulous calibration has been performed with similar condition as in the field (i.e., with a gradient of viscosity due to cooler outer surface), the measurements are often biased by the outer cooler surface of the lava. More sophisticated penetrometers such as the Mark 2 employed by Pinkerton and Sparks (1978) can prevent the effect of the cooler lava surface.

A falling sphere method was employed by Shaw et al. (1968), and although he obtained a measurement at a low strain rate (0.004 s^{-1}), this method can only be employed on a stable lava lake of sufficient depth, and with a suitable thick crust. Nonetheless this is currently the only way to measure the viscosity of silicate liquids under pressure in the laboratory (Kono, 2018).

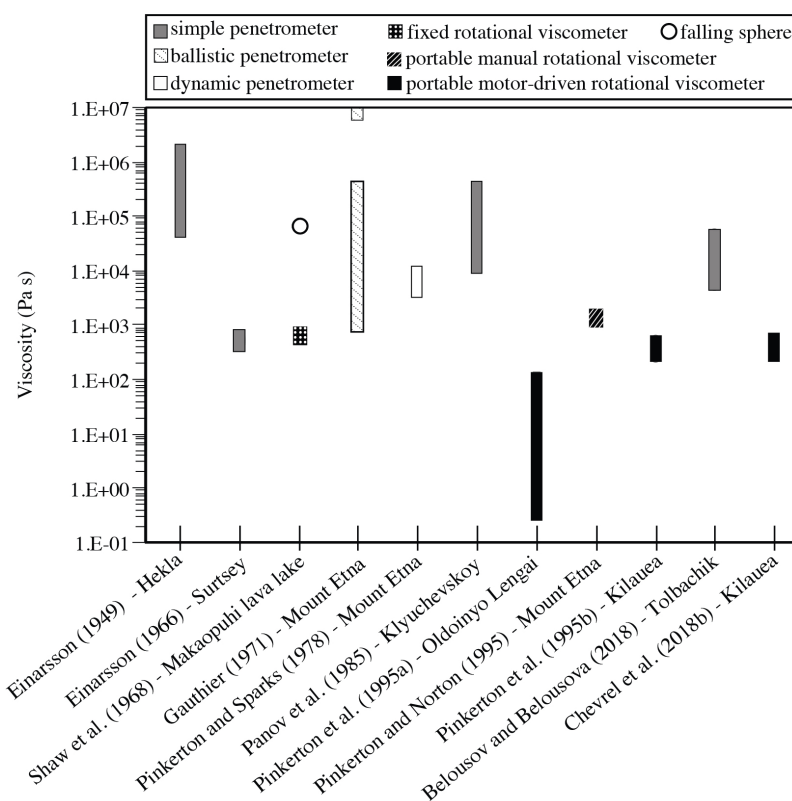


Figure 4: Viscosity range measured during field campaigns. The boxes are grey-shaded according to the type of viscometers.

Rotational viscometry appears to be the most promising approach for field measurement on low viscosity lava ($< 10^4 \text{ Pa s}$; Figure 4). This instrument can apply various strain rates ($0.1 - > 5 \text{ s}^{-1}$; Figure 4) that permit the construction of full flow curves (Pinkerton

and Norton, 1995; Pinkerton et al. 1995b). In 1968, the rotational viscometer set up by Shaw et al. (1968) provided accurate measurements. However it is unsuitable for active lava flows that are in constant motion and often have short-lived instable levées. In 1994, Pinkerton (1994) built the first generation of portable, motor-driven, rotational viscometer. The measurements presented in Chevrel et al. (2018a) showed that this instrument, equipped with a new torque sensor communication system, continues to work well, but has some important limitations. These are 1) it was not possible to achieve low strain rate ($< 1 \text{ s}^{-1}$) because of limiting low rotation speeds and 2) this instrument is bulky and heavy ($>15 \text{ kg}$) and requires two people to handle it and a third person to monitor the results, which hinders the easy, fast and flexible handling required in the field around an active lava.

We suggest that a combination of two instruments, a rotational viscometer for low viscosity range ($< 10^4 \text{ Pa s}$) and a dynamic penetrometer for higher viscosities ($10^3 - 10^6 \text{ Pa s}$), may therefore be the most appropriate procedure. For lavas with higher viscosity ($> 10^6 \text{ Pa s}$) no field instruments are available for such measurement. Besides, field viscometry will be extremely challenging because such flows are usually ‘a‘ā to blocky with an outer thick fragmented crust that is impossible to approach and penetrate. In addition, the time required to measure viscosity may expose the operator to unacceptable risk from falling blocks.

4.2 Comparison of the rheological results in different geological settings

4.2.1 *Hawaiian lavas*

Using rotational viscometers, the viscosity of Hawaiian lavas measured in the field at temperatures between $1146 \text{ }^{\circ}\text{C}$ and $1130 \text{ }^{\circ}\text{C}$, falls within the range $1.5 \times 10^3 \text{ Pa s}$ at strain rates less than 1 s^{-1} to $2.6 \times 10^2 \text{ Pa s}$ at strain rates higher than 1 s^{-1} (Figure 5). The measurements of Shaw et al. (1968) were performed at low strain rate ($0.1 - 1 \text{ s}^{-1}$), and although the data were first fitted with a Bingham model, later Heslop et al. (1989) showed that a power law model would be more appropriate. Pinkerton et al. (1995) applied low-to-moderate strain rates ($0.2 - 3.2 \text{ s}^{-1}$) that also showed the pseudo-plastic behavior of the lava. In contrast, Chevrel et al. (2018a) performed measurements at higher strain rates ($>1 \text{ s}^{-1}$) and although they could be fitted with a power law, the Newtonian rheological model provided a better fit at $3.8 \times 10^2 \text{ Pa s}$. The similarity between the collected samples and the viscosities obtained at unit strain rate in 1994 and 2016, using almost the same instrument but 22 years apart, is consistent with the fact that temperature, composition and texture (amount of bubbles and crystals) was similar in the two field studies. These viscosities are lower than the values

obtained by Shaw et al. (1968), which is consistent with a higher temperature, lower crystal content and higher content of deformable bubble in the lava from Pinkerton et al. (1995) and Chevrel et al. (2018b). The value obtained by Shaw et al. (1968) using a falling sphere revealed even higher viscosities ($> 10^4$ Pa s) at very low strain rates (0.004 s $^{-1}$). All three data sets suggest a pseudo-plastic behavior of Hawaiian lavas under these conditions (Figure 5).

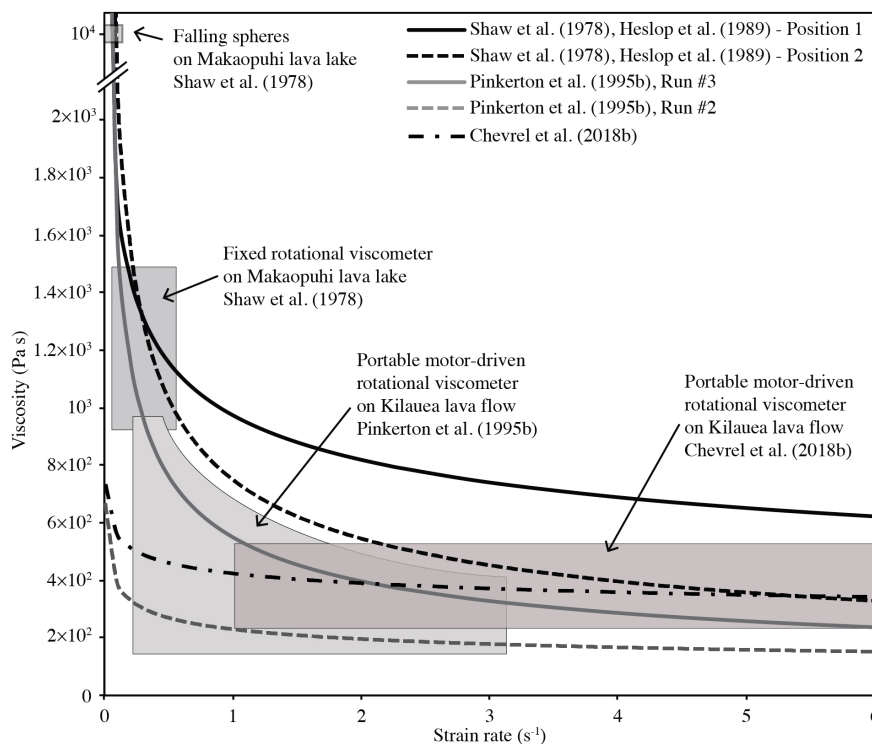


Figure 5: Variation of viscosity with strain rate for Hawaiian lavas as obtained from field viscometry. Boxes represent the measured range of viscosity and strain rate and curves are best fits as given by the different studies.

Among these field experiments at Hawaii, none have directly recorded a yield strength. The estimation of yield strength given by Shaw et al. (1968) was made by fitting the data to a Bingham model. According to laboratory experiments of Hawaiian lavas at subliquidus condition (Ryerson et al. 1988; Sehlke et al., 2014), yield strength may appear with crystallization but should be less than 200 Pa for the crystal content of the lavas measured in the field (< 25 vol. %). Unfortunately, this relatively low yield strength is, to date, difficult, if not impossible, to measure using current field instruments. Further measurements at low shear stresses and low strain rates are needed to determine whether yield

strength can develop. Until then a power law model is considered to be the most appropriate model to characterize the behavior of Hawaiian lava at temperatures above 1130 °C (Figure 5).

The agreement between field measurements and the model-based viscosity using textural and chemical characterization shows our capacity of estimating and measuring three-phase mixture viscosity. However, this is only true for a given temperature and only when an exhaustive sample analyses is generated. Further measurements on pāhoehoe lava need to be performed so as to test the sensitivity of viscosity to the effect small thermal, physical of chemical changes within a lava field.

4.2.2 Etnean lavas

At Mount Etna, measurements were performed on ‘a‘ā type lava flows using different instruments including penetrometers and a manually-operated rotating viscometer (Figure 4). The measured viscosities (either on lava blocks or on channelized lava) range mostly between 10^3 Pa s and 10^4 Pa s. Gauthier (1973) recorded very high viscosities ($> 10^7$ Pa s) using a ballistic penetrometer but these high values are unduly influenced by the cooler outer crust (penetration depth was only 1 cm) and therefore do not represent the flowing lava interior. The viscosities measured by Pinkerton and Sparks (1978) using the Mark 2 penetrometer were higher (9.4×10^3 Pa s) than those measured by Pinkerton and Norton (1995) using a rotational viscometer (approx. 1.3×10^3 Pa s). This difference is considered to be a result of a combination of factors, including different eruptive temperatures (1086 °C in 1975 compared with 1095 °C in 1983), different crystal content (45 vol. % in 1975 and < 40 vol. % 1983), and lower strain rates used in 1975 ($0 - 0.15$ s⁻¹) compared with 1983 ($0.7 - 1.4$ s⁻¹). Pinkerton and Sparks (1978) measured lava yield strength using various instruments and they found a clear correlation with temperature and consequently crystallinity.

Although the rheological properties of Etnean lavas are now well constrained from laboratory experiments (e.g. Pinkerton and Norton, 1995; Vona et al., 2011; Vona and Romano, 2013), there are not enough field measurements to build flow curves under field conditions.

4.2.3 Kamchatka and Icelandic lavas

The measurements on basaltic-andesite lavas from Klyuchevskoy and Tolbachik showed that the pāhoehoe lobes measured by Belousov and Belousova (2018) have slightly lower viscosities than the ‘a‘ā flow measured by Panov et al. (1988): $0.5 - 5 \times 10^4$ Pa s and $0.11 - 3.6 \times 10^5$ Pa s, respectively. However, the investigation by Belousov and Belousova

(2018) at Tolbachik, revealed that the lava traveling within the ‘a‘ā channel was slightly less viscous than the early erupted pāhoehoe lava. This is consistent with some observations at Hawaii, where pāhoehoe flows formed from the rupture of ‘a‘ā front flow (Hon et al., 2003). In general the Kamchatka pāhoehoe lobes are more viscous than Hawaiian lavas, which is attributed to the lower temperature, higher silica content and higher crystallinity of the former in comparison to the later.

Finally, Einarsson (1949; 1966) measured viscosities at Surtsey as low as 5×10^2 Pa s and up to 1.5×10^6 Pa s at Hekla both using the same penetrometer. However the value at Surtsey was challenging to measure, as the rod sank too quickly under its own weight. Unfortunately, there are no other field measurements to compare with. This highlights the need for more data to build flow curves and determine the lava rheological behavior from these field locations in Russia and Iceland.

4.3 Future requirements for field viscometry

Reducing errors associated with field measurements requires accurate sensors as well as meticulous setup and calibration, which is difficult to achieve in the field where conditions are more complex than in the lab. Field measurements are always constrained by the lava’s thermal dynamics. To reduce the effects of crust formation during measurements the instrument needs to be pre-heated and inserted into fresh molten lava, emerging through breaches in the crust, or at the breaking point of pāhoehoe lobes, where little-to-no crust is present. The time of the measurements then needs to be always shorter than crust formation. Another procedure to minimize the effect of crust formation is to use viscometers like the “Mark 2” (Pinkerton and Sparks, 1978), which allow triggering the sensor once the lava isothermal core is reached. A detailed engineering drawing of the Mark 2 can be found in Pinkerton (1978; Figure 2). Note also that interpretation of the results is non-trivial, but pre- and post- calibration in fluids of different viscosity can be used to validate the results from an analysis of the raw data. Gauthier (1971) proposed a set up similar in sophistication to that used in the laboratory, where the viscometer head would float on the lava surface, protected from radiant heat by a cooling carapace. This would drive a sensitive spindle plunged in the lava. Although this instrument may produce useful data, it would be time-consuming and expensive to build, and there would be a high risk of losing it during utilization in the field.

Future viscometers need to be robust, light enough to be carried over rough ground to remote locations, easily mounted and easy to handle, ideally by one person. Additionally, in order to capture the full rheological behavior of lava, viscometers need to apply low strain

rates ($< 1 \text{ s}^{-1}$) and record low shear stresses ($< 200 \text{ Pa}$). This will constrain the dimensions of the shear vane or spindle, torque sensor capability and motor power. Using newer (electronically controlled) technology and a lighter and modern motorized system, a new generation of rotational viscometer seems to be the most suitable way forwards toward future measurements on basaltic lava.

The material used for field viscometer needs to be resistant to high temperatures. In the laboratory, crucibles containing the lava and rotating spindles are usually made of platinum-rhodium alloy or alumina ceramics. However, at the torques applied in the field, the former does not supply sufficient mechanical strength and may, therefore, deform too easily and the latter may break. Instead low carbon stainless steel alloy is often favored. This material is resistant both mechanically and to heat and seems to have the best value for money. Although its composition (of mainly iron) may contaminate the lava, the degree of contamination is considered to be insignificant considering the timescale of the measurements, although this should be investigated in detail during future experiments.

Finally, and most importantly, viscosity measurements must be made in combination with temperature measurements and lava sampling for textural analysis. The rheological evolution of lava during flow is controlled by the cooling rate (Giordano et al., 2007), which also controlled the crystal size distribution (Vetere et al., 2015). Recent laboratory-based work has shown that viscometry associated with synchronous temperature measurement is the key for understanding lava flow behavior at conditions pertinent to nature (Kolzenburg et al., 2017, 2016). This also includes changes in shear rate and oxygen fugacity (Kolzenburg et al., 2018a, 2018b). Future field viscometers should therefore incorporate a thermocouple.

Textural and petrographic analysis of the sample is the key to understanding how crystal and bubble content affect rheology during lava emplacement. The molten lava must always be sampled and quenched rapidly to conserve the texture at the location of the viscosity measurement. Future field campaigns should focus on measuring lava properties, temperature and lava texture as a function of distance from the vent to the front and across the flow, in order to map lava rheology in 4D through the flow.

5 Conclusion

Field viscometry at active lava flows is the only way to capture the rheology of lava in its natural state. It is also a very challenging method to employ in the field. Since the 1940's there are eleven studies. These field experiments and their results highlight that they have

considerable potential, but the definitive study has yet to be undertaken. The most important aspect is the choice and design of the viscometer. The rotational viscometer seems to be the most appropriate instrument for low viscosity lava ($< 10^4 - 10^5$ Pa s) as it allows a large range of strain rate to be applied (0.1 to > 5 s⁻¹). For higher viscosity lava ($10^5 - 10^6$ Pa s), well-calibrated penetrometers designed to avoid the effects of the cooler outer lava surface are suitable. Above 10^6 Pa s measurement is not viable, as penetration becomes impossible. Using field measurements, flow curves could be established only for Hawaiian lavas and revealed a pseudo-plastic behavior. Further works still remain to be carried out on other basaltic volcanoes to ensure a full understanding of the lava rheological behavior under field conditions.

If suitable precautions are taken during measurements and post-processing of data, field viscometry in combination with simultaneous temperature measurements and laboratory studies of quenched samples collected at each measurement site will improve our understanding of evolving lava viscosity as a function of cooling rate, degassing and crystallisation. This will create the data required for the development of flow emplacement models. Future improvements include adding thermal sensors and building lighter and electronically controlled viscometers with simple operating systems that can achieve a wide range of strain- and stress-rates.

Acknowledgement

We warmly acknowledge M. R. James for useful discussions and for assisting with equipment refinement. We acknowledge S. Kolzenburg for thorough reviews and Gillian R. Foulger for handling the manuscript. This research was partly financed by the Auvergne fellowship (Labex ClerVolc) attributed to M.O.Chevrel and by the Agence National de la Recherche through the project LAVA (Program: DS0902 2016; Project: ANR-16 CE39-0009, <http://www.agence-nationale-recherche.fr/Projet-ANR-16-CE39-0009>). This is ANR-LAVA contribution no. 10 and ClerVolc publication n°349.

References

Avard, G., Whittington, A.G., 2012. Rheology of arc dacite lavas: experimental determination at low strain rates. *Bull. Volcanol.* 74, 1039–1056. <https://doi.org/10.1007/s00445-012-0584-2>

- 773 Bagdassarov, N.S., Dingwell, D.B., 1993. Deformation of foamed rhyolites under internal and
774 external stresses: An experimental investigation. *Bullettin Volcanol.* 55, 147–154.
775 <https://doi.org/10.1007/BF00301512>
- 776 Bagdassarov, N.S., Dingwell, D.B., 1992. A rheological investigation of vesicular rhyolite. *J.*
777 *Volcanol. Geotherm. Res.* 50, 307–322. [https://doi.org/10.1016/0377-0273\(92\)90099-Y](https://doi.org/10.1016/0377-0273(92)90099-Y)
- 778 Bagdassarov, N.S., Dingwell, D.B., Webb, S.L., 1994. Viscoelasticity of crystal-bearing and
779 bubble-bearing rhyolite melts. *Phys. Earth Planet. Inter.* 83.
780 [https://doi.org/10.1016/0031-9201\(94\)90066-3](https://doi.org/10.1016/0031-9201(94)90066-3)
- 781 Bagdassarov, N.S., Pinkerton, H., 2004. Transient phenomena in vesicular lava flows based
782 on laboratory experiments with analogue materials. *J. Volcanol. Geotherm. Res.* 132,
783 115–136.
- 784 Balmforth, N.J., Craster, R. V., Rust, A.C., Sassi, R., 2007. Viscoplastic flow over an inclined
785 surface. *J. Nonnewton. Fluid Mech.* 142, 219–243.
786 <https://doi.org/10.1016/j.jnnfm.2006.07.013>
- 787 Barnes, H.A., 1989. *An Introduction to Rheology*, Rheology series 3. U.S. and Canada,
788 Elsevier Science.
- 789 Belousov, A., Belousova, M., 2018. Dynamics and viscosity of ‘a‘ā and pāhoehoe lava flows
790 of the 2012-2013 eruption of Tolbachik volcano, Kamchatka (Russia). *Bull. Volcanol.*
791 80. <https://doi.org/doi.org/10.1007/s00445-017-1180-2>
- 792 Bilotta, G., Herault, A., Cappello, A., Ganci, G., Negro, C. Del, 2014. GPUSPH: a Smoothed
793 Particle Hydrodynamics model for the thermal and rheological evolution of lava flows,
794 in: Harris, A.J.L., De Groeve, T., Garel, F., Carn, S.A. (Eds.), *Detecting, Modelling and*
795 *Responding to Effusive Eruptions*. Geological Society, London, pp. 387–408.
796 <https://doi.org/10.1144/SP426.24>
- 797 Bottinga, Y., Weill, D.F., 1972. The viscosity of magmatic silicate liquids: A model for
798 calculation. *Am. J. Sci.* 272, 438–475. <https://doi.org/10.2475/ajs.272.5.438>
- 799 Bottinga, Y., Weill, D.F., 1970. Density of liquid silicate systems calculated from partial
800 molar volumes of oxide components. *Am. J. Sci.* 269(2), 169.
801 <https://doi.org/10.2475/ajs.269.2.169>
- 802 Caricchi, L., Giordano, D., Burlini, L., Ulmer, P., 2008. Rheological properties of magma
803 from the 1538 eruption of Monte Nuovo (Phlegrean Fields, Italy): An experimental
804 study. *Chem. Geol.* 256, 158–171. <https://doi.org/10.1016/j.chemgeo.2008.06.035>
- 805 Cashman, K. V., Thornber, C., Kauahikaua, J.P., 1999. Cooling and crystallization of lava in

- open channels, and the transition of pāhoehoe lava to ‘a‘ā. *Bull. Volcanol.* 61, 306–323.
<https://doi.org/10.1007/s004450050299>
- Castruccio, A., Contreras, M.A., 2016. The influence of effusion rate and rheology on lava flow dynamics and morphology: A case study from the 1971 and 1988-1990 eruptions at Villarrica and Lonquimay volcanoes, Southern Andes of Chile. *J. Volcanol. Geotherm. Res.* 327, 469–483. <https://doi.org/10.1016/j.jvolgeores.2016.09.015>
- Castruccio, A., Rust, A.C., Sparks, R.S.J., 2013. Evolution of crust- and core-dominated lava flows using scaling analysis. *Bull. Volcanol.* 75, 681. <https://doi.org/10.1007/s00445-012-0681-2>
- Castruccio, A., Rust, A.C., Sparks, R.S.J., 2010. Rheology and flow of crystal-bearing lavas: Insights from analogue gravity currents. *Earth Planet. Sci. Lett.* 297, 471–480. <https://doi.org/10.1016/j.epsl.2010.06.051>
- Champallier, R., Bystricky, M., Arbaret, L., 2008. Experimental investigation of magma rheology at 300 MPa: From pure hydrous melt to 76 vol.% of crystals. *Earth Planet. Sci. Lett.* 267, 571–583. <https://doi.org/10.1016/j.epsl.2007.11.065>
- Chester, D.K., Duncan, A.M., Guest, J.E., Kilburn, C.R.J., 1986. Mount Etna: The anatomy of a volcano. Springer Netherlands. <https://doi.org/10.1007/978-94-009-4079-6>
- Chevrel, M.O., Cimarelli, C., DeBiasi, L., Hanson, J.B., Lavallée, Y., Arzilli, F., Dingwell, D.B., 2015. Viscosity measurements of crystallizing andesite from Tungurahua volcano (Ecuador). *Geochemistry, Geophys. Geosystems* 16, 870–889. <https://doi.org/10.1002/2014GC005661>
- Chevrel, M.O., Guilbaud, M.-N., Siebe, C., 2016. The ~AD 1250 effusive eruption of El Metate shield volcano (Michoacán, Mexico): Magma source, crustal storage, eruptive dynamics, and lava rheology. *Bull. Volcanol.* 78, 1–28. <https://doi.org/10.1007/s00445-016-1020-9>
- Chevrel, M.O., Harris, A.J.L., James, M.R., Calabrò, L., Gurioli, L., Pinkerton, H., 2018b. The viscosity of pāhoehoe lava: In situ syn-eruptive measurements from Kilauea, Hawaii. *Earth Planet. Sci. Lett.* 493, 161–171. <https://doi.org/10.1016/j.epsl.2018.04.028>
- Chevrel, M.O., Labroquere, J., Harris, A.J.L., Rowland, S.K., 2018a. PyFLOWGO: an open-source platform for simulation of channelized lava thermo-rheological properties. *Comput. Geosci.* 111, 167–180. <https://doi.org/10.1016/j.cageo.2017.11.009>
- Chevrel, M.O., Platz, T., Hauber, E., Baratoux, D., Lavallée, Y., Dingwell, D.B., 2013. Lava flow rheology: A comparison of morphological and petrological methods. *Earth Planet.*

- 839 Sci. Lett. 384, 102–120. <https://doi.org/10.1016/j.epsl.2013.09.022>
- 840 Cigolini, C., Borgia, A., Casertano, L., 1984. Intra-crater activity, ‘a’-block lava, viscosity
841 and flow dynamics: Arenal Volcano, Costa Rica. *J. Volcanol. Geotherm. Res.* 20, 155–
842 176. [https://doi.org/10.1016/0377-0273\(84\)90072-6](https://doi.org/10.1016/0377-0273(84)90072-6)
- 843 Cimarelli, C., Costa, A., Mueller, S., Mader, H.M., 2011. Rheology of magmas with bimodal
844 crystal size and shape distributions: Insights from analog experiments. *Geochem.*
845 *Geophys. Geosyst.* 12, Q07024. <https://doi.org/10.1029/2011GC003606>
- 846 Coppola, D., Laiolo, M., Franchi, A., Massimetti, F., Cigolini, C., Lara, L.E., 2017.
847 Measuring effusion rates of obsidian lava flows by means of satellite thermal data. *J.*
848 *Volcanol. Geotherm. Res.* 347, 82–90. <https://doi.org/10.1016/j.jvolgeores.2017.09.003>
- 849 Cordonnier, B., Hess, K.U., Lavalle, Y., Dingwell, D.B., 2009. Rheological properties of
850 dome lavas: Case study of Unzen volcano. *Earth Planet. Sci. Lett.* 279, 263–272.
851 <https://doi.org/10.1016/j.epsl.2009.01.014>
- 852 Costa, A., Caricchi, L., Bagdassarov, N.S., 2009. A model for the rheology of particle-bearing
853 suspensions and partially molten rocks. *Geochemistry Geophys. Geosystems* 10,
854 Q03010. <https://doi.org/10.1029/2008GC002138>
- 855 Crisci, G.M., Di Gregorio, S., Pindaro, O., Ranieri, G.A., 1986. Lava flow simulation by a
856 discrete cellular model: first implementation. *Int. J. Model. Simul.* 6, 137–140.
- 857 Crisp, J., Cashman, K. v., Bonini, J.A., Hougen, S.B., Pieri, D.C., 1994. Crystallization
858 history of the 1984 Mauna Loa lava flow. *J. Geophys. Res.* 99, 7177–7198.
859 <https://doi.org/10.1029/93JB02973>
- 860 Dingwell, D.B., 1986. Viscosity-temperature relationships in the system Na₂Si₂O₅-
861 Na₄Al₂O₅. *Geochim. Cosmochim. Acta* 50, 1261–1265.
- 862 Einarsson, T., 1966. Studies of temperature, viscosity, density and some types of materials
863 produced in the Surtsey eruption, Surtsey Research Program Report.
- 864 Einarsson, T., 1949. The flowing lava. Studies of its main physical and chemical properties.,
865 in: *The Eruption of Hekla 1947-1948. Soc Scientiarum Islandica, Reykjavik*, pp. 1–70.
- 866 Einstein, A., 1906. Eine neue Bestimmung der Molekuldimensionen. *Ann. Phys.* 19, 289.
- 867 Fink, J.H., Zimbelman, J.R., 1986. Rheology of the 1983 Royal Gardens basalt flows, Kilauea
868 Volcano, Hawaii. *Bull. Volcanol.* 48, 87–96. <https://doi.org/10.1007/BF01046544>
- 869 Ganci, G., Vicari, A., Cappello, A., Del Negro, C., 2012. An emergent strategy for volcano
870 hazard assessment: From thermal satellite monitoring to lava flow modeling. *Remote*
871 *Sens. Environ.* 119, 197–207. <https://doi.org/10.1016/j.rse.2011.12.021>

- Gauthier, F., 1973. Field and laboratory studies of the rheology of Mount Etna lava. *Philos. Trans. R. Soc. London A Math. Phys. Eng. Sci.* 274, 83–98.
- Gauthier, F., 1971. Etude comparative des caractéristiques rhéologiques des laves basaltiques en laboratoire et sur le terrain. PhD, Univ. Paris-Sud, Fac. des Sci. d'Orsay.
- Giordano, D., Dingwell, D.B., 2003. Non-Arrhenian multicomponent melt viscosity: a model. *Earth Planet. Sci. Lett.* 6556, 1–13. [https://doi.org/10.1016/S0012-821X\(03\)00042-6](https://doi.org/10.1016/S0012-821X(03)00042-6)
- Giordano, D., Polacci, M., Longo, A., Papale, P., Dingwell, D.B., Boschi, E., Kasereka, M., 2007. Thermo-rheological magma control on the impact of highly fluid lava flows at Mt. Nyiragongo. *Geophys. Res. Lett.* 34.
- Giordano, D., Russell, J.K., Dingwell, D.B., 2008. Viscosity of magmatic liquids: A model. *Earth Planet. Sci. Lett.* 271, 123–134. <https://doi.org/10.1016/j.epsl.2008.03.038>
- Griffiths, R.W., 2000. The Dynamics of Lava Flows. *Annu. Rev. Fluid Mech.* 32, 377–518. <https://doi.org/10.1146/annurev.fluid.32.1.477>
- Guilbaud, M.N., Blake, S., Thordarson, T., Self, S., 2007. Role of Syn-eruptive Cooling and Degassing on Textures of Lavas from the ad 1783-1784 Laki Eruption, South Iceland. *J. Petrol.* 48, 1265–1294. <https://doi.org/10.1093/petrology/egm017>
- Harris, A.J.L., Allen, J.S., 2008. One-, two- and three-phase viscosity treatments for basaltic lava flows. *J. Geophys. Res.* 113, B09212. <https://doi.org/10.1029/2007JB005035>
- Harris, A.J.L., Bailey, J., Calvari, S., Dehn, J., 2005. Heat loss measured at a lava channel and its implications for down-channel cooling and rheology. *Geol. Soc. Am. Spec. Pap.* 396, 125–146. [https://doi.org/10.1130/2005.2396\(09\)](https://doi.org/10.1130/2005.2396(09)).
- Harris, A.J.L., Flynn, L.P., Matías, O., Rose, W.I., 2002. The thermal stealth flows of Santiaguito dome, Guatemala: Implications for the cooling and emplacement of dacitic block-lava flows. *Bull. Geol. Soc. Am.* 114, 533–546. [https://doi.org/10.1130/0016-7606\(2002\)114<0533:TTSFOS>2.0.CO;2](https://doi.org/10.1130/0016-7606(2002)114<0533:TTSFOS>2.0.CO;2)
- Harris, A.J.L., Flynn, L.P., Matias, O., Rose, W.I., Cornejo, J., 2004. The evolution of an active silicic lava flow field: an ETM + perspective 135, 147–168. <https://doi.org/10.1016/j.jvolgeores.2003.12.011>
- Harris, A.J.L., Rowland, S.K., 2009. Effusion Rate Controls on Lava Flow Length and the Role of Heat Loss: A Review. *Leg. Georg. P.L. Walker, Spec. Publ. IAVCEI. Eds Hoskuldsson A, Thordarson T, Larsen G, Self S, Rowl. S. Geol. Soc. London.* 2, 33–51.
- Harris, A.J.L., Rowland, S.K., 2001. FLOWGO: a kinematic thermo-rheological model for lava flowing in a channel. *Bull. Volcanol.* 63, 20–44.

- <https://doi.org/10.1007/s004450000120>
- Herault, A., Bilotta, G., Vicari, A., Rustico, E., Del Negro, C., 2011. Numerical simulation of lava flow using a GPU SPH model. Del Negro, C. Gresta, S. Lava Flow Invasion Hazard Map Mt. Etna Methods its Dyn. Updat. Ann. Geophys. 54.
- Herault, A., Bilotta, G., Vicari, A., Rustico, E., Del Negro, C., 2009. Forecasting lava flow hazards during the 2006 Etna eruption: Using the MAGFLOW cellular automata model. J. Volcanol. Geotherm. Res. 112, 78–88. <https://doi.org/10.1016/j.cageo.2007.10.008>
- Heslop, S.E., Wilson, L., Pinkerton, H., Head, J.W., 1989. Dynamics of a confined lava flow on Kilauea Volcano, Hawaii. Bull. Volcanol. 51, 415–432.
- Hess, K.-U., Dingwell, D.B., 1996. Viscosities of hydrous leucogranitic melts: {A non-Arrhenian model}. Am. Mineral. 81, 1297–1300.
- Hidaka, M., Goto, A., Umino, S., Fujita, E., 2005. VTFS project: development of the lava flow simulation code LavaSIM with a model for three-dimensional convection, spreading, and solidification. Geochemistry, Geophys. Geosystems 6, Q07008.
- Hon, K., Gansecki, C., Kauahikaua, J., 2003. The transition from 'a'ā to pāhoehoe crust on flows emplaced during the Pu'u 'Ō'ō-Kūpaianaha eruption. USGS Prof. Pap. 1676 89–103. [https://doi.org/10.1016/0003-6870\(73\)90259-7](https://doi.org/10.1016/0003-6870(73)90259-7)
- Hui, H., Zhang, Y., 2007. Toward a general viscosity equation for natural anhydrous and hydrous silicate melts. Geochim. Cosmochim. Acta 71, 403–416.
- Hulme, G., 1974. The Interpretation of Lava Flow Morphology. Geophys. J. R. Astron. Soc. 39, 361–383.
- Ishibashi, H., Sato, H., 2007. Viscosity measurements of subliquidus magmas: Alkali olivine basalt from the Higashi-Matsuura district, Southwest Japan. J. Volcanol. Geotherm. Res. 160, 223–238.
- James, M.R., Pinkerton, H., Robson, S., 2007. Image-based measurement of flux variation in distal regions of active lava flows. Geochemistry, Geophys. Geosystems 8. <https://doi.org/10.1029/2006GC001448>
- Jeffreys, H., 1925. The flow of water in an inclined channel of rectangular section. Philos. Mag. serie 6, 4, 293,793-807.
- Kelfoun, K., Vargas, S.V., 2016. VolcFlow capabilities and potential development for the simulation of lava flows, in: Harris, A.J.L., De Groeve, T., Garel, F., Carn, S.A. (Eds.), Detecting, Modelling and Responding to Effusive Eruptions. Geological Society, London, pp. 337–343. <https://doi.org/10.1144/SP426.8>

- 938 Kerr, R.C., Lyman, A.W., 2007. Importance of surface crust strength during the flow of the
939 1988-1990 andesite lava of Lonquimay Volcano, Chile. *J. Geophys. Res.* 112, B03209.
- 940 Keszthelyi, L., Self, S., 1998. Some physical requirements for the emplacement of long
941 basaltic lava flows. *J. Geophys. Res.* B11, 27,447-27,464.
- 942 Kilburn, C.R.J., Lopes, R.M.C., 1991. General patterns of flow field growth: 'A'a and blocky
943 lavas. *J. Geophys. Res.* 96, 19721–19732. <https://doi.org/10.1029/91jb01924>
- 944 Klein, J., Mueller, S.P., Helo, C., Schweitzer, S., Gurioli, L., Castro, J.M., 2018. An expanded
945 model and application of the combined effect of crystal-size distribution and crystal
946 shape on the relative viscosity of magmas. *J. Volcanol. Geotherm. Res.* 357, 128–133.
947 <https://doi.org/10.1016/j.jvolgeores.2018.04.018>
- 948 Kolzenburg, S., Di Genova, D., Giordano, D., Hess, K.-U., Dingwell, D.B., 2018a. The effect
949 of oxygen fugacity on the rheological evolution of crystallizing basaltic melts. *Earth*
950 *Planet. Sci. Lett.* 487, 21–32. <https://doi.org/10.1016/j.epsl.2018.01.023>
- 951 Kolzenburg, S., Giordano, D., Cimorelli, S., Dingwell, D.B., 2016. In situ thermal
952 characterization of cooling/crystallizing lavas during rheology measurements and
953 implications for lava flow emplacement. *Geochim. Cosmochim. Acta* 195, 244–258.
- 954 Kolzenburg, S., Giordano, D., Hess, K.-U., Dingwell, D.B., 2018b. Shear-rate Dependent
955 Disequilibrium Rheology and Dynamics of Basalt Solidification. *Geophys. Res. Lett.*
956 <https://doi.org/doi.org/10.1029/2018GL077799>
- 957 Kolzenburg, S., Giordano, D., Thordarson, T., Hoskuldsson, A., Dingwell, D.B., 2017. The
958 rheological evolution of the 2014/2015 eruption at Holuhraun, central Iceland. *Bull.*
959 *Volcanol.* 79.
- 960 Kolzenburg, S., Jaenicke, J., Münzer, U., Dingwell, D.B., 2018c. The effect of inflation on
961 the morphology-derived rheological parameters of lava flows and its implications for
962 interpreting remote sensing data - A case study on the 2014/2015 eruption at Holuhraun,
963 Iceland. *J. Volcanol. Geotherm. Res.* 357, 200–212.
964 <https://doi.org/10.1016/j.jvolgeores.2018.04.024>
- 965 Kono, Y., 2018. Viscosity Measurement, in: *Magmas Under Pressure*. Elsevier, pp. 261–280.
966 <https://doi.org/10.1016/B978-0-12-811301-1.00010-1>
- 967 Krauskopf, K.B., 1948. Lava Mouvement at Paricutin Volcano, Mexico. *Geol. Soc. Am.*
968 *Bull.* 12, 1267–1284.
- 969 Krieger, I.M., Dougherty, T.J., 1959. A Mechanism for Non-Newtonian Flow in Suspensions
970 of Rigid Spheres. *J. Rheol. (N. Y. N. Y.)* 3, 137.

- 971 Larson, R.G., 1999. The structure and rheology of complex fluids. Oxford University Press,
972 New York.
- 973 Lavallée, Y., Hess, K.-U., Cordonnier, B., Dingwell, D.B., 2007. Non-Newtonian rheological
974 law for highly crystalline dome lavas. *Geology* 35, 843–846.
- 975 Lavallée, Y., Varley, N.R., Alatorre-Ibargüengoitia, M.A., Hess, K.-U., Kueppers, U.,
976 Mueller, S., Richard, D., Scheu, B., Spieler, O., Dingwell, D.B., 2012. Magmatic
977 architecture of dome-building eruptions at Volcán de Colima, Mexico. *Bull. Volcanol.*
978 74, 249–260.
- 979 Le Losq, C., Neuville, D.R., Moretti, R., Kyle, P.R., Oppenheimer, C., 2015. Rheology of
980 phonolitic magmas - the case of the Erebus lava lake. *Earth Planet. Sci. Lett.* 411, 53–61.
981 <https://doi.org/10.1016/j.epsl.2014.11.042>
- 982 Lefler, E., 2011. Genauigkeitsbetrachtung bei der Ermittlung rheologischer Parameter von
983 Lavaströmen aus Fernerkundungsdaten. Berlin, Freie Universität.
- 984 Lejeune, A.M., Bottinga, Y., Trull, T.W., P., R., 1999. Rheology of bubble-bearing magmas.
985 *Earth Planet. Sci. Lett.* 166, 71–84.
- 986 Lenk, R.S., 1967. A Generalized Flow Theory. *J. Appl. Polym. Sci.* 11, 1033–1042.
- 987 Lev, E., James, M.R., 2014. The influence of cross-sectional channel geometry on rheology
988 and flux estimates for active lava flows. <https://doi.org/10.1007/s00445-014-0829-3>
- 989 Lipman, P.W., Banks, N.G., 1987. Aa flow dynamics, Mauna Loa 1984. *U.S. Geol. Surv.*
990 *Prof. Pap* 1350 1527–1567.
- 991 Lipman, P.W., Banks, N.G., Rhodes, J.M., 1985. Degassing-induced crystallization of
992 basaltic magma and effects on lava rheology. *Nature* 317, 604–607.
- 993 Llewellyn, E.W., Manga, M., 2005. Bubble suspension rheology and implications for conduit
994 flow. *J. Volcanol. Geotherm. Res.* 143, 205–217.
- 995 Lunne, T., Robertson P.K., Powell, J.J.M., 1997. Cone Penetration Testing in Geotechnical
996 Practice. Blackie Academic/Chapman-Hall, U.K.
- 997 Mader, H.M., Llewellyn, E.W., Mueller, S.P., 2013. The rheology of two-phase magmas: A
998 review and analysis. *Bull. Volcanol.* 257, 135–158.
- 999 Manga, M., Castro, J., Cashman, K. V, M., L., 1998. Rheology of bubble-bearing magmas. *J.*
1000 *Volcanol. Geotherm. Res.* 87, 15–28.
- 1001 Maron, S.H., Pierce, P.E., 1956. Application of Ree-Eyring generalized flow theory to
1002 suspensions of spherical particles. *J. Colloid Sci.* 11, 80–95.
- 1003 Moitra, P., Gonnermann, H.M., 2015. Effects of crystal shape- and size-modality on magma

- 1004 rheology. *Geochemistry, Geophys. Geosystems* 16, 1–26.
- 1005 Moore, H.J., 1987. Preliminary estimates of the rheological properties of 1984 Mauna Loa
1006 Lava. *U.S. Geol. Surv. Prof. Pap.* 1350 99, 1569–1588.
- 1007 Moore, H.J., Schaber, G.G., 1975. An estimate of the yield strength of the Imbrium flows.
1008 *Proceeding Lunar Sci. Conf.* 6th, 101–118.
- 1009 Mossoux, S., Saey, M., Bartolini, S., S., P., Canters, F., Kervyn, M., 2016. Q-LAVHA: A
1010 flexible GIS plugin to simulate lava flows. *Comput. Geosci.* 97, 98–109.
- 1011 Mueller, S., Llewellyn, E.W., Mader, H.M., 2010. The rheology of suspensions of solid
1012 particles. *Philos. Trans. R. Soc. Lond. A* 466, 1201–1228.
- 1013 Nichols, R.L., 1939. Viscosity of Lava. *J. Geol.* 47, 290–302.
- 1014 Norton, G., Pinkerton, H., 1997. Rheological properties of natrocarbonatite lavas from
1015 Oldoinyo Lengai, Tanzania. *Eur. J. Mineral.* 9, 351–364.
- 1016 Panov, V.K., Slezin, Y.B., Storcheus, A. V, 1988. Mechanical properties of lavas extruded in
1017 the 1983 Predskazannyi eruption (Klyuchevskoy volcano). *Volcanol. Seismol.* 7, 25–37.
- 1018 Panov, V.K., Slezin, Y.B., Storcheus, A. V, 1985. Mechanical properties of lavas of flank
1019 eruption Predskazanny (Predicted), 1983, Klyuchevskoy volcano. *J. Volcanol. Seismol.*
1020 *Russ.* 1, 21–28.
- 1021 Phan-Thien, N., Pham, D.C., 1997. Differential multiphase models for polydispersed
1022 suspensions and particulate solids. *J. Nonnewton. Fluid Mech.* 72, 305–318.
- 1023 Pinkerton, H., 1994. Rheological and related properties of lavas, in: F. Dobran (Ed.), *Etna:*
1024 *Magma and Lava Flow Modeling and Volcanic System Definition Aimed at Hazard*
1025 *Assessment. Global Volcanic And Environmental System Simulation*, pp. 76–89.
- 1026 Pinkerton, H., 1978. *Methods of Measuring the Rheological Properties of Lava.* University of
1027 Lancaster.
- 1028 Pinkerton, H., Herd, R.A., Kent, R.M., Wilson, L., 1995b. Field measurements of the
1029 rheological properties of basaltic lavas. *Lunar Planet. Sci.* XXVI, 1127–1128.
- 1030 Pinkerton, H., Norton, G., 1995. Rheological properties of basaltic lavas at sub-liquidus
1031 temperatures: laboratory and field measurements on lavas from Mount Etna. *J. Volcanol.*
1032 *Geotherm. Res.* 68, 307–323.
- 1033 Pinkerton, H., Norton, G., 1983. A comparison of calculated and measured rheological
1034 properties of crystallizing lavas in the field and in the laboratory, in: *Lunar and Planetary*
1035 *Science XXIV.* pp. 1149–1150.
- 1036 Pinkerton, H., Norton, G.E., Dawson, J.B., Pyle, D.M., 1995a. Field observations and

- measurements of the physical properties of Oldoinyo Lengai alkali carbonatite lavas, November 1988, in: Bell, K., Keller, J. (Eds.), IAVCEI Proceedings in Volcanology 4. Carbonatite Volcanism of Oldoinyo Lengai - Petrogenesis of Natrocarbonatite. Springer-Verlag, Berlin, pp. 23–36.
- Pinkerton, H., Sparks, R.S.J., 1978. Field measurements of the rheology of lava. *Nature* 276, 383–385.
- Pinkerton, H., Stevenson, R.J., 1992. Methods of determining the rheological properties of magmas at sub-liquidus temperatures. *J. Volcanol. Geotherm. Res.* 53, 47–66.
- Pinkerton, H., Wilson, L., 1994. Factor controlling the lengths of channel-fed lava flows. *Bull. Volcanol.* 6, 108–120.
- Pistone, M., Caricchi, L., Ulmer, P., Burlini, L., Ardia, P., Reusser, E., Marone, F., L., A., 2012. Deformation experiments of bubble- and crystal-bearing magmas: Rheological and microstructural analysis. *J. Geophys. Res.* 117, B05208.
- Pistone, M., Caricchi, L., Ulmer, P., Reusser, E., Ardia, P., 2013. Rheology of volatile-bearing crystal mushes: Mobilization vs. viscous death. *Chem. Geol.* 345, 16–39. <https://doi.org/10.1016/j.chemgeo.2013.02.007>
- Pistone, M., Cordonnier, B., Ulmer, P., Caricchi, L., 2016. Rheological flow laws for multiphase magmas: An empirical approach. *J. Volcanol. Geotherm. Res.* 321, 158–170. <https://doi.org/10.1016/j.jvolgeores.2016.04.029>
- Plechov, P., Blundy, J., Nekrylov, N., Melekhova, E., Shcherbakov, V., Tikhonova, M.S., 2015. Petrology and volatile content of magmas erupted from Tolbachik Volcano, Kamchatka, 2012–13. *J. Volcanol. Geotherm. Res.* 307, 182–199. <https://doi.org/10.1016/j.jvolgeores.2015.08.011>
- Ramsey, M., Chevrel, M.O., Coppola, D., Harris, A.J.L., 2019. The influence of emissivity on the thermo-rheologic al modeling of the channelized lava flows at Tolbachik volcano. *Ann. Geophys.* 61.
- Rh  ty, M., Harris, A.J.L., Villeneuve, N., Gurioli, L., M  dard, E., Chevrel, M.O., Bach  lery, P., 2017. A comparison of cooling-limited and volume-limited flow systems: Examples from channels in the Piton de la Fournaise April 2007 lava-flow field. *Geochemistry, Geophys. Geosystems* 18, 3270–3291. <https://doi.org/10.1002/2017GC006839>
- Riker, J.M., Cashman, K. V., Kauahikaua, J.P., Montierth, C.M., 2009. The length of channelised lava flows: insight from the 1859 eruption of Mauna Loa Volcano, Hawaii. *J. Volcanol. Geotherm. Res.* 183, 139–156.

- Robert, B., Harris, A., Gurioli, G., Medard, E., Sehlke, A., Whittington, A., 2014. Textural and rheological evolution of basalt flowing down a lava channel. *Bull. Volcanol.* 76, 824.
- Rose, W.I., 1973. Pattern and mechanism of volcanic activity at the Santiaguito Volcanic Dome, Guatemala. *Bull. Volcanol.* 37, 73–94. <https://doi.org/10.1007/BF02596881>
- Rust, A.C., Manga, M., 2002. Bubble shapes and orientations in low Re simple shear flow. *Journal Colloid Interface Sci.* 249, 476–480.
- Ryerson, F.J., Weed, H.C., Piwinski, A.J., 1988. Rheology of subliquidus magmas: Picritic compositions. *J. Geophys. Res.* 93, 3421–3436.
- Saar, M.O., Manga, M., 1999. Permeability-porosity relationship in vesicular basalts. *Geophys. Res. Lett.* 26, 111–114.
- Sato, H., 2005. Viscosity measurement of subliquidus magmas: 1707 basalt of Fuji volcano. *J. Mineral. Petrol. Sci.* 100, 133–142.
- Sehlke, A., Whittington, A., Robert, B., Harris, A.J.L., Gurioli, L., Médard, E., 2014. Pahoehe to 'a'a transition of Hawaiian lavas: an experimental study. *Bull. Volcanol.* 76, 876.
- Sehlke, A., Whittington, A.G., 2016. The viscosity of planetary tholeiitic melts: A configurational entropy model. *Geochim. Cosmochim. Acta* 191, 277–299.
- Shaw, H.R., 1972. Viscosities of magmatic silicate liquids: An empirical method of prediction. *Am. J. Sci.* 272, 870–893.
- Shaw, H.R., Wright, T.L., Peck, D.L., Okamura, R., 1968. The Viscosity of Basaltic Magma: An analysis of Field Measurements in Makaopuhi Lava Lake, Hawaii. *Am. J. Sci.* 266, 225–264.
- Smith, J. V, 2000. Textural evidence for dilatant (shear thickening) rheology of magma at high crystal concentrations. *J. Volcanol. Geotherm. Res.* 99, 1–7.
- Smith, J. V, 1997. Shear thickening dilatancy in crystal-rich flows. *J. Volcanol. Geotherm. Res.* 79, 1–8.
- Soldati, A., Sehlke, A., Chigna, G., Whittington, A., 2014. Field and experimental constraints on the rheology of arc basaltic lavas: the January 2014 Eruption of Pacaya (Guatemala). *Bull. Volcanol.* 78.
- Sólnes J, Á. Ásgeirsson, B. Bessason, and F. Sigmundsson. Náttúruvá Á Íslandi, Eldgos og Jarðskjálftar. Reykjavík: Viðlagatrygging/ Háskólaútgáfan, 2013
- Soule, S.A., Cashman, K.V., Kauahikaua, J.P., 2004. Examining flow emplacement through

- 1103 the surface morphology of three rapidly emplaced, solidified lava flows, Kīlauea
 1104 Volcano, Hawai'i. *Bull. Volcanol.* 66, 1–14. <https://doi.org/10.1007/s00445-003-0291-0>
- 1105 Spera, F.J., Borgia, A., Strimple, J., Feigenson, M., 1988. Rheology of melts and magmatic
 1106 suspensions I. Design and calibration of a concentric cylinder viscometer with
 1107 application to rhyolitic magma. *J. Geophys. Res.* 93, 10273–10294.
- 1108 Stein, D.J., Spera, F.J., 1998. New high-temperature rotational rheometer for silicate melts,
 1109 magmatic suspensions, and emulsions. *Rev. Sci. Instrum.* 69, 3398–3402.
 1110 <https://doi.org/doi:10.1063/1.1149106>
- 1111 Stein, D.J., Spera, F.J., 1992. Rheology and microstructure of magmatic emulsions: Theory
 1112 and experiments. *J. Volcanol. Geotherm. Res.* 49, 157–174.
- 1113 Vetere, F., Iezzi, G., Behrens, H., Holtz, F., Ventura, G., Misiti, V., Cavallo, A., Mollo, S.,
 1114 Dietrich, M., 2015. Glass forming ability and crystallisation behaviour of sub-alkaline
 1115 silicate melts. *Earth-Science Rev.* 150, 25–44.
 1116 <https://doi.org/10.1016/j.earscirev.2015.07.001>
- 1117 Vetere, F., Sato, H., Ishibashi, H., De Rosa, R., Donato, P., Ishebashi, H., De Rosa, R.,
 1118 Donato, P., 2013. Viscosity changes during crystallization of a shoshonitic magma: new
 1119 insights on lava flow emplacement. *J. Mineral. Petrol. Sci.* 108, 144–160.
 1120 <https://doi.org/10.2465/jmps.120724>
- 1121 Vicari, A., Bilotta, G., Bonfiglio, S., Cappello, A., Ganci, G., Herault, A., Rustico, E., Gallo,
 1122 G., Del Negro, C., 2011. Lav@hazard: A web-gis interface for volcanic hazard
 1123 assessment. *Ann. Geophys.* 54, 662–670. <https://doi.org/10.4401/ag-5347>
- 1124 Vicari, A., Herault, A., Del Negro, C., Coltelli, M., Marsella, M., Proietti, C., 2007. Modeling
 1125 of the 2001 lava flow at Etna volcano by a Cellular Automata approach. *Environ. Model.*
 1126 *Softw.* 22, 1465–1471.
- 1127 Vona, A., Di Piazza, A., Nicotra, E., Romano, C., Viccaro, M., Giordano, G., 2017. The
 1128 complex rheology of megacryst-rich magmas: The case of the mugearitic “cicirara” lavas
 1129 of Mt. Etna volcano. *Chem. Geol.* 458, 48–67.
 1130 <https://doi.org/10.1016/j.chemgeo.2017.03.029>
- 1131 Vona, A., Romano, C., 2013. The effects of undercooling and deformation rates on the
 1132 crystallization kinetics of Stromboli and Etna basalts. *Contrib. to Mineral. Petrol.* 166,
 1133 491–509. <https://doi.org/10.1007/s00410-013-0887-0>
- 1134 Vona, A., Romano, C., Dingwell, D.B., Giordano, D., 2011. The rheology of crystal-bearing
 1135 basaltic magmas from Stromboli and Etna. *Geochim. Cosmochim. Acta* 3214–3236.

- 1136 Vona, A., Romano, C., Giordano, D., Russell, J.K., 2013. The multiphase rheology of
1137 magmas from Monte Nuovo (Campi Flegrei, Italy). *Chem. Geol.* 346, 213–227.
1138 <https://doi.org/10.1016/j.chemgeo.2012.10.005>
- 1139 Vona, A., Ryan, A.G., Russell, J.K., Romano, C., 2016. Models for viscosity and shear
1140 localization in bubble-rich magmas. *Earth Planet. Sci. Lett.* 449, 26–38.
1141 <https://doi.org/10.1016/j.epsl.2016.05.029>
- 1142 Wadge, G., Lopes, R.M.C., 1991. The lobes of lava flows on Earth and Olympus Mons, Mars.
1143 *Bull. Volcanol.* 6, 10–24.
- 1144 Walker, G.P.L., 1973. Lengths of lava flows. *Philos. Trans. R. Soc. London* 274, 107–118.
- 1145 Woodcock, D., Harris, A., 2006. The dynamics of a channel-fed lava flow on Pico Partido
1146 volcano, Lanzarote. *Bull. Volcanol.* 69, 207–215. [https://doi.org/10.1007/s00445-006-](https://doi.org/10.1007/s00445-006-0068-3)
1147 [0068-3](https://doi.org/10.1007/s00445-006-0068-3)
- 1148